

Graphic Presentation of Directional Data from the Wadi Al Qattarah Formation, Wadi Al Aqar Quarry, Al Jabal Al Akhdar, NE Libya: An Approach for Outcrop Characterization, Geostatistics, and Inferred Paleogeography

Omar B. Elfigih¹, Osama A. Alshireef²

¹ Professor in Petroleum Geology, Department of Earth Sciences, Faculty of Science, University of Benghazi, Libya,

² Geologist, Geological Department, Exploration Division, Sirte Oil Company, Brega, Libya,

-----ABSTRACT-----

Abstract: Geostatistical analysis through computed mean vector azimuth (MVA) for the studied cross-bedding structures in oolitic limestones of the Wadi Al Qattarah Formation in the Wadi Al Aqar-NE Libya was done by using the recommended standard formula [$MVA = \tan^{-1}(\frac{\sum \sin\theta}{\sum \cos\theta})$]. Graphic presentation of the studied cross-bedding directions has revealed a strong unidirectional orientation of cross-beds with minor reversals at some localities. In each unit, the primary mode is to the southeast, whereas the secondary mode is essentially asymmetrical about the mode. The strike of the cross-bedding sets in these deposits is normal to this trend. These data indicate that marine paleocurrent systems during the deposition of the oolitic limestones of the Wadi Al Qattarah Formation moved back and forth perpendicular to the shore and were probably the result of the strong ebb and flow of tides. The framework of these marine paleocurrents has suggested the inferred paleogeography of the Wadi Al Qattarah Formation in Wadi Al Aqar Quarry, in which the dispersal of the oolitic and skeletal limestone ridges in the southeast direction (ebb tide direction), changing to lagoonal settings in the northwestern and northeastern directions (flood tide direction).

Keywords: Geostatistics, Graphic presentation, Directional data, Outcrop characterization, Cross bedding, Paleocurrent, Wadi Al Qattarah Formation, Wadi Al Aqar, Ebb tide, Flood tide, Paleogeography.

Date of Submission: 12-05-2025

Date of acceptance: 26-05-2025

I. Introduction

Paleocurrent analysis involves using sedimentary structures as paleocurrent indicators (cross beddings, asymmetrical ripple marks, channels, and clasts imbrication) to determine the direction of flow or orientation of flow like that of a river, a group of streams within a basin, the wind direction within a region, or the direction of oceanic currents. Individual sedimentary structures tell you the flow direction at that geographic point and at that instant in time but in solving true regional scale problems we need to look statistically at populations of sedimentary structures [1]. These will give us a collective average of the current directions or paleoflows within a region over some time [2], [3].

Symmetrical and asymmetrical cross beddings may be encountered in the studied facies. Good exposure of the oolitic limestone of the Late Miocene Wadi Al Qattarah Formation in the study area can be divided into several depositional facies each of which has a designated sedimentary structure that could be used to define the paleoflow direction of that facies during the depositional time.

1.1 Location map of the study area

Field investigation centered on Wadi Al Qattarah Formation outcrops in Wadi Al Aqar Quarry which is located in the northern part of Al Jabal Al Akhdar region between longitude 20° 43' 54" E and latitude 32° 29' 49" N (Fig. 1).

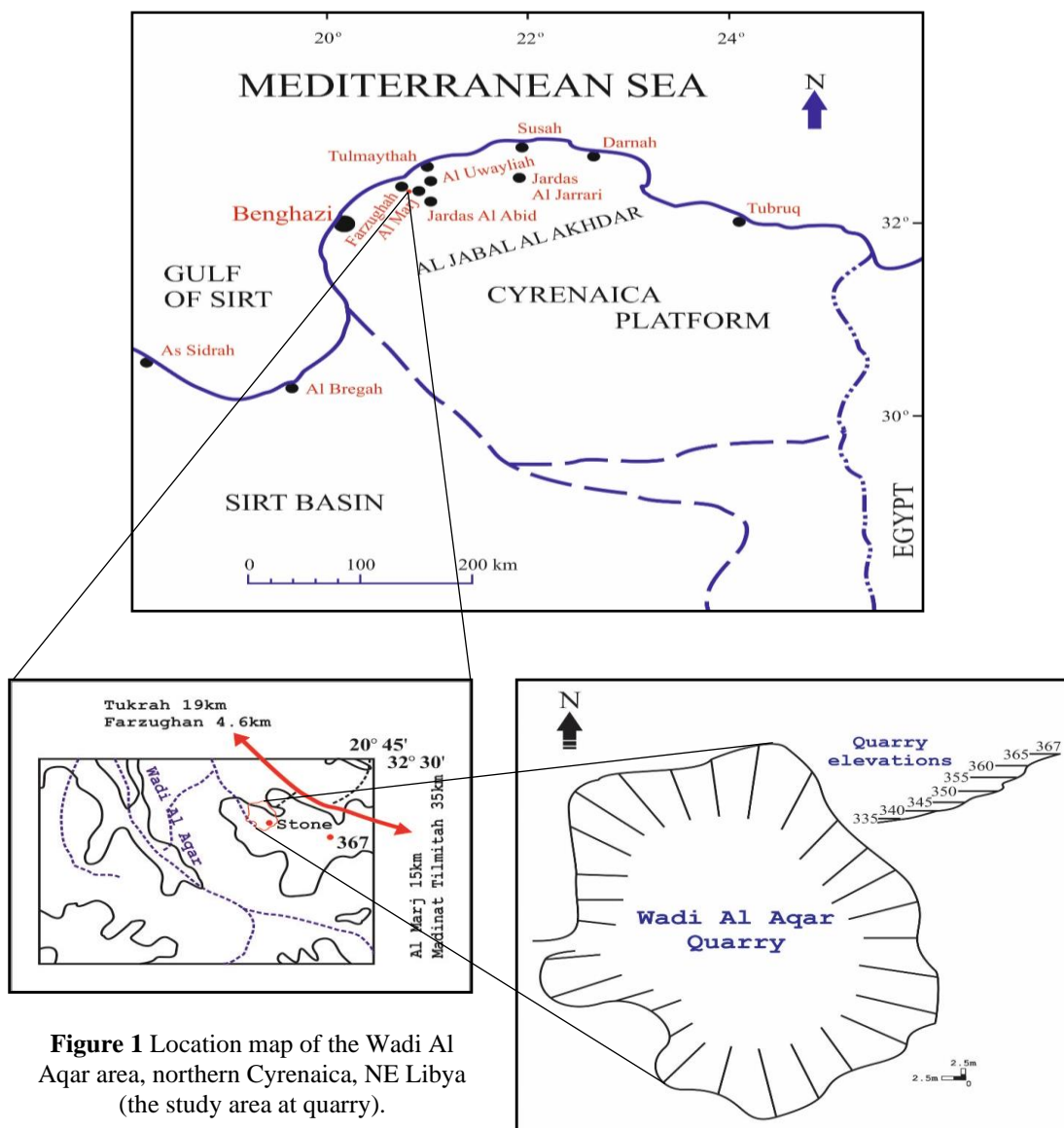


Figure 1 Location map of the Wadi Al Aqar area, northern Cyrenaica, NE Libya (the study area at quarry).

1.2 Objectives

The main purpose of the study is to know the paleocurrent direction of the Wadi Al Qattarah Formation in Wadi Al Aqar Quarry, in an attempt to determine the degree of preferred orientation of possible marine paleoflows during Wadi Al Qattarah Formation depositional time and the relationship of these directional flows to inferred paleogeography.

1.3 Previous work

Geological previous studies in Miocene rocks were established by Klen (1974) [4] who subdivide the Ar Rajmah Formation into Benghazi and Wadi Al Qattarah Members. El Hawat (1980) studied the Middle Miocene sequence of the Wadi Al Qattarah Member of the Ar Rajmah Formation and suggested that the depositional model of this Member is deposited under intertidal and storm environments.

During mapping by the Industrial Research Centre (IRC) further to the south and west of the coastal area, Francis and Issawi (1977) [5], Mazhar and Issawi (1977) [6], and Swedan and Issawi (1977) [7] raised Ar Rajmah into a group, but they divided it into three formations. These are Masus, Al Sceleidima, and Benghazi Formations. Banerjee (1980) subsequently rejected this subdivision and priority was given to the formation status of Ar Rajmah. The discovery of a major regional unconformity dividing the succession into two correlatable units by El Hawat and Salem (1987) [8], led to the establishment of two separate sequences. The

lower sequence, Benghazi Member, was assigned to the Middle Miocene, while the upper sequence was assigned to the Upper Miocene based on the sedimentological and sequence stratigraphic attributes.

For the same, the sequence stratigraphic and sedimentologic reasoning Ar Rajmah has been raised here into a group, and these two Middle-Upper Miocene members are raised to formations status El Hawat, 1986 a [9], 1986b [10]; El Hawat *et al.*, 1993 [11].

Abdulsamad and Barbieri (1999) [12] discussed the distribution of the foraminifera and the palaeoenvironmental significance of the Eocene-Miocene succession in NE Libya. Abdulsamad *et al.* (2009) [13] published a stratigraphic review of the Eocene to Miocene rock units in the Al Jabal Al Akhdar, NE Libya. Abdulsamad and El Zanati (2013) [14] prepared a paper on the Miocene benthic foraminifera from the Soluq area, NE Libya: biostratigraphy and environmental significance.

Abdulsamad and Tmalla (2013) [15] discussed the systematic paleontology of Oligocene-Miocene planktonic foraminifera from NE Libya. Amrouni *et al.* (2013) [16] published the sedimentology and sequence stratigraphy of the Middle to Late Miocene, Al-Jabal Al-Khadar uplift, and Soluq trough, Cyrenaican NE Libya. Amrouni and Pope (2015) [17] studied the sequence stratigraphy, chemostratigraphy, and diagenesis of the Cyrenaican Miocene carbonate-evaporite successions, in NE Libya.

Muftah *et al.* (2015) [18] wrote about the utilization of the observed geological features in differentiating the exposed rock units in Al Jabal al Akhdar, Libya. Abdulsamad *et al.* (2018) [19] studied stratigraphy and larger benthic foraminifera of Middle Eocene to Middle Miocene rocks along the Tobruk-Al Bardia scarps, northeastern Cyrenaica, Libya. Elfigih *et al.* (2018) [20] described the lithostratigraphic correlation of the Middle Eocene-Upper Miocene rocks between sectors (1-5), Tansulukh Region, Al Jabal Al Akhdar NE Libya: An integrating study from previously studied wadies.

The study of paleocurrent indicators has been demonstrated in several studies and publications including mathematical techniques for paleocurrent analysis: treatment of directional data (Rao and Sengupta, 1970 [21]). Also, Shah *et al.* (2009) [22] described the paleocurrent analysis of the Dhok Pathan Formation, from Thathi northeastern Potwar Dist. Rawalpindi.

Parks (1970) [23] studied the paleocurrent analysis of sedimentary crossbed data with graphic output using three integrated computer programs. Tucker (2003 [24]) has a simple article about palaeocurrent analysis in the sedimentary rocks in the field book. There is a good explanation in the applied sedimentology book concerning the palaeocurrent analysis Selley, 2000) [25].

Paleocurrent analysis was performed giving cognizance to the precepts of Potter and Pettijohn (1978) [2] and Boggs (2006) [3]. The sedimentary structures were also utilized following the procedures enlisted by Tucker (2011) [26]. However, there is no paleocurrent study has been conducted in Wadi Al Aqar Quarry, and this is why this study was suggested.

II. Geological Setting

Tectonically, Cyrenaica is located in northeastern Libya on the North African coast. It consists of two distinct tectonic provinces separated by a hinge line called the Cyrenaican fault system. These provinces are the mobile north Cyrenaica inverted basin, referred to as Al Jabal Al Akhdar, and the more stable Cyrenaica platform to the south (Fig. 2). The northern mobile belt area has been influenced by the Tethys tectonic activities and events since its opening during the Jurassic. It was subsequently shaped by the reversal of the Eurasian and African plate movement that led to the subduction of the latter beneath the former from the Upper Cretaceous to the present [27].

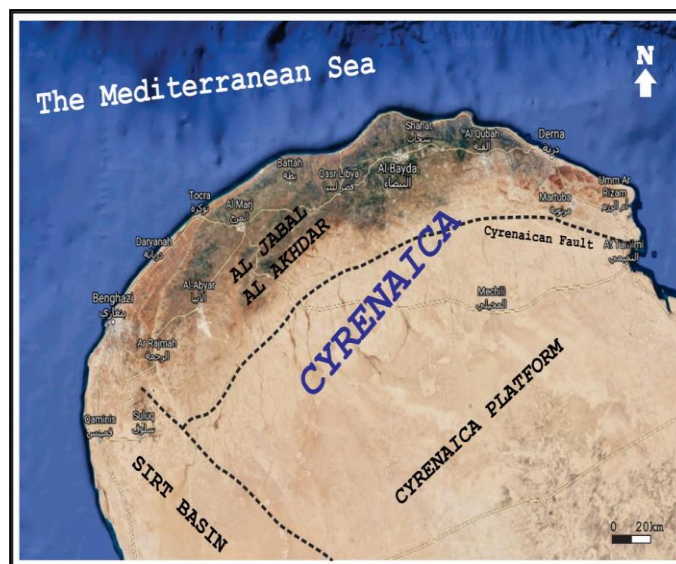


Figure 2 Land sat image of northern Cyrenaica showing main tectonic provinces [27] (updated by google map, 2020).

Generally, during the Late Oligocene-Early Miocene time Al Jabal Al Akhdar anticlinorium formed as a chain of elevated Cretaceous, Early Tertiary Island in the Miocene sea, the Oligocene-Miocene boundary was found to be erosional everywhere in Libya [28].

Stratigraphically, the exposed surface rocks (Fig. 3) of the Cyrenaica Platform range from Cretaceous to Late Miocene [27]. The Eocene to Late Miocene rocks of Cyrenaica (Fig. 3) are subdivided into five unconformity-bounded sequences [28], [27]. The exposures of the Al Jabal Al Akhdar, north Cyrenaica, are mainly shallow to deep marine carbonate rocks. However, the Miocene is a mixed shallow marine carbonate and lagoonal rock type [28].

The stratigraphic subdivision of the Miocene rock sequence was regarded as the Middle Miocene Ar Rajmah Formation [29] and was later subdivided into the Benghazi and Wadi Al Qattarah Members [4]. Later in the northern part of Cyrenaica, the Benghazi and Wadi Al Qattarah Members were raised to formations and Ar Rajmah was raised to group status in Cyrenaica (Fig. 3) based on sedimentological and sequence stratigraphic analysis [27].

The Early Miocene Al Faidyah Formation is characterized by green glauconite at its basal contact overlain by marly wackestone to packstone [1], [13], [28], and [30]. Fore-slope to deep shelf open marine facies mainly composed of coral boundstone and skeletal wackestone [8], [27] of the Middle Miocene Benghazi Formation record a transgression that covered almost the entirety of the Cyrenaica Platform [28].

Subsequently, The Late Miocene (Tortonian) sequence of Wadi Al Qattarah Formation in Al Jabal Al Akhdar is composed primarily of Tortonian cross-bedded oolitic and bioclastic grainstone shoals of barrier islands overlain by Messinian restricted carbonate and back-barrier lagoonal mudstone, stromatolites, and interbedded evaporite rocks [28] deposited through major regression that coincided with the separation between the Tethys and the Paratethys, and the Messinian salinity crisis of the Mediterranean [28] and marked regional disconformity surfaces.

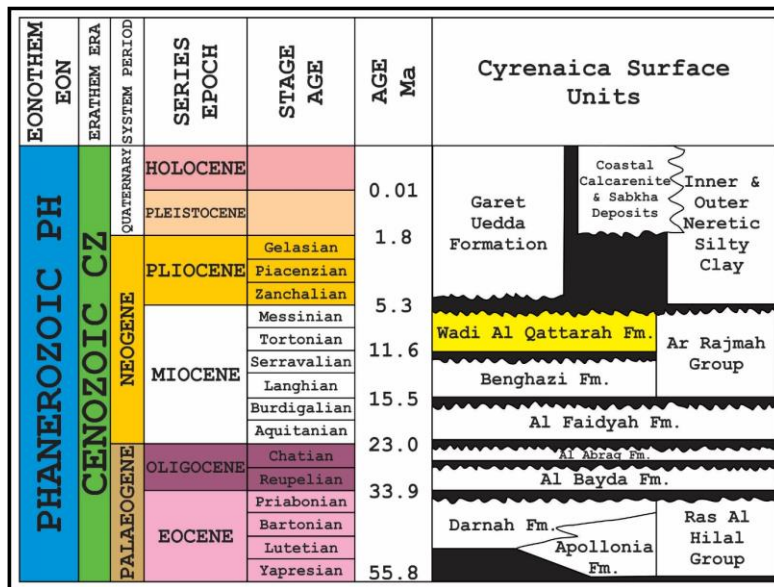


Figure 3 Part of surface stratigraphic units of the exposed Tertiary Formations of Cyrenaica, Al Jabal Al Akhdar, NE Libya [27](El Hawat and Abdulsamad,

III. Methodology

This study focuses on the Wadi Al Qattarah Formation in Wadi Al Aqar Quarry, Al Jabal Al Akhdar, NE Libya (Fig. 1). A good exposure up to 36m thick provides an exceptional setting of carbonate rocks to be studied through their paleocurrent data.

3.1 Measured Outcrop Sections

Outcrop-logged sections were considered the main method in this study. A total of 8 vertical measured sections of approximately 176.5m were logged over an area of 1776 m² (37m x 48m) in Wadi Al Aqar Quarry (Fig. 4).

The litho-type composite section of the vertical stratigraphic sequence (Fig. 5) of the Late Miocene Wadi Al Qattarah Formation in the study area at Wadi Al Aqar Quarry is composed of 36 m sequential carbonate rocks with bioturbated oolitic in parts muddy limestone at the base to planar oolitic wackestone-packstone, to grainstone-packstone low-angle cross-bedded oolitic channel fill and trough cross-bedded oolitic channel complex, to planar cross-bedded massive oolitic grainstone packstone-wackestone and back shoal herringbone cross-bedding in the top part (Fig.5).

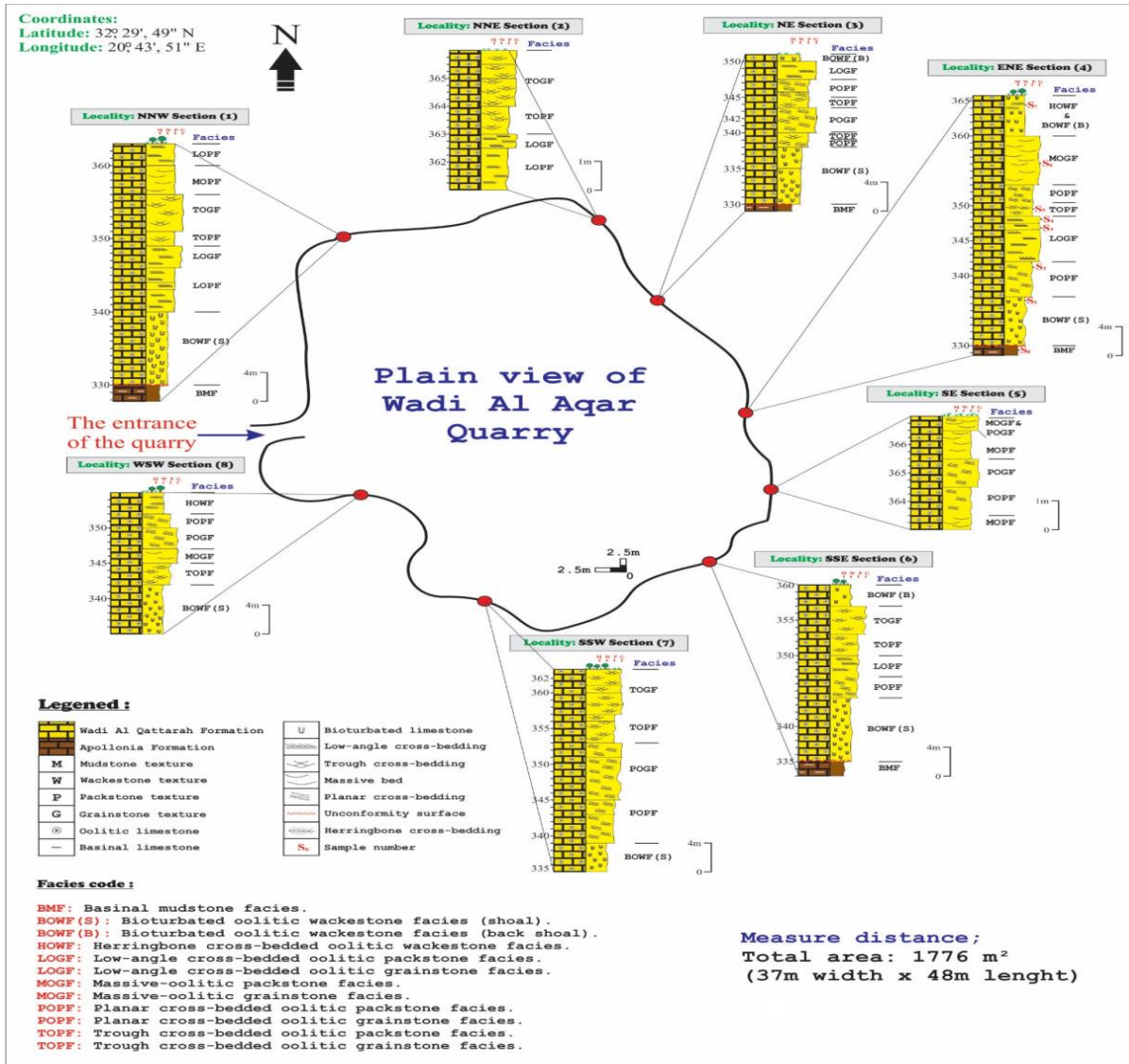


Figure 4 Locations of measured sections and the identified facies of Wadi Al Qattarah Formation in Wadi Al Aqar Quarry, Al Jabal Al Akhdar, NE Libya.

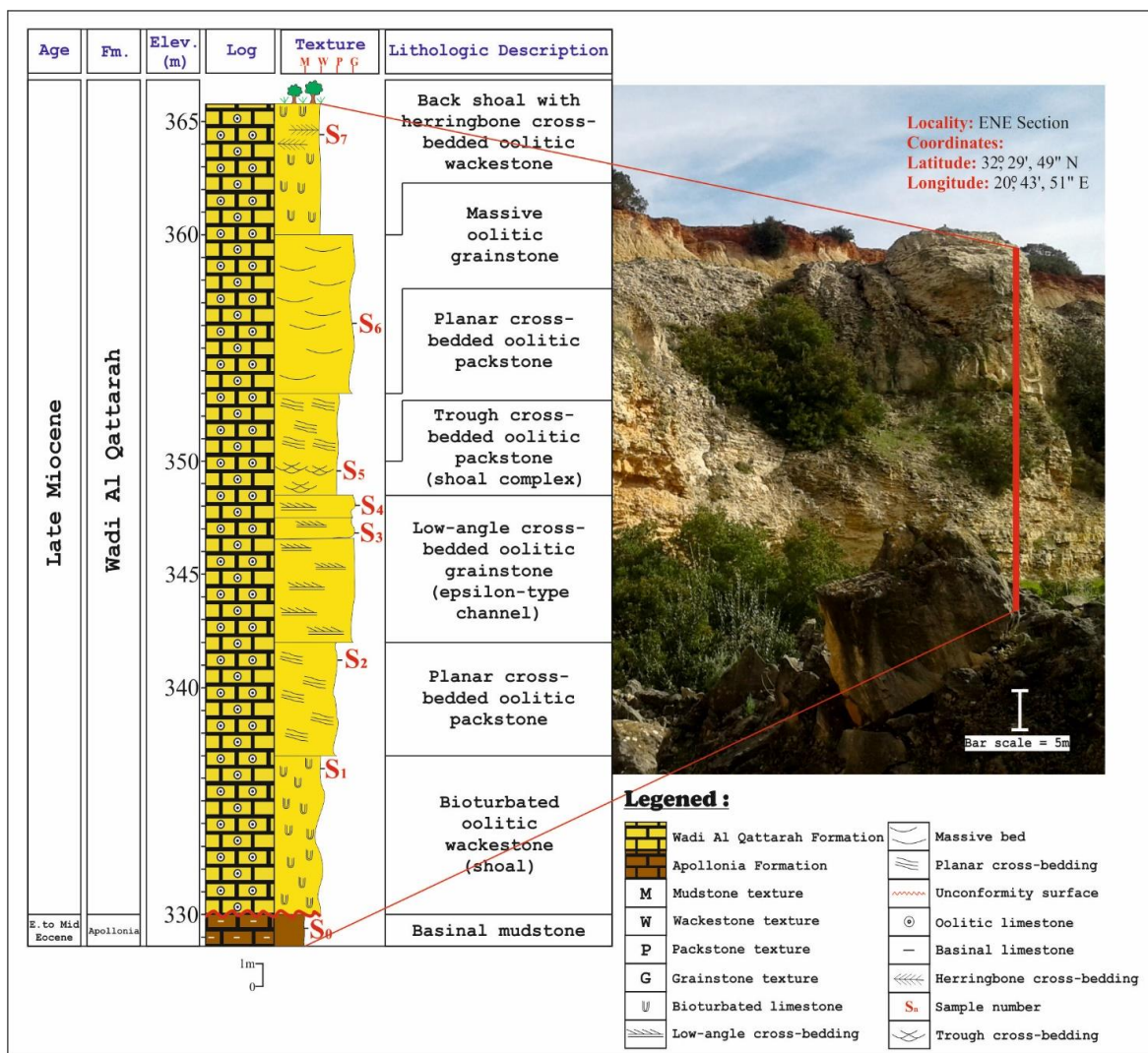


Figure 5 Showing the location of the litho-type section in the Quarry of Wadi Al Aqar.

3.2 Field Collection of Paleocurrent Data

In the field, paleocurrent data were measured with the Brunton compass on the orientation of the observed structure. For cross-beddings point down-stream, we record the down current directions, for those which may give us trough cross-bedding of stream orientation we record the bearing for that trend expressed as azimuth degrees. This is recorded in the field book.

The beds of the studied outcrop from which we are making paleocurrent measurements are semi-horizontally laying and characterized by low tectonic dip values not exceeding 15 degrees, which indicate no effect of tilting or major tectonic on the area. Hence, no correction for the beds dip or plunge is necessary [22], [31].

A total of 335 paleocurrent measurements (Tables 1-8) were selected for the collection of data from different paleocurrent indicators, such as low-angle cross-bedding associated with oolitic packstone-grainstone facies (LOPF-LOGF) in sections (1 & 2), oolitic grainstone facies (LOGF) in sections (3 & 4) and oolitic packstone facies (LOPF) in section (6), whereas trough cross-bedding associated with oolitic packstone-grainstone facies (TOPF-TOGF) in sections (1, 2, 6 & 7) and oolitic packstone facies (TOPF) in sections (3, 4 & 8). Planar cross-bedding associated with oolitic packstone-grainstone facies (POPF-POGF) in sections (3, 5, 7 & 8) and oolitic packstone facies (POPF) in sections (4 & 6), while other distinct cross-bedding in the field are herringbones style associated with oolitic wackestone facies (HOWF) (Fig. 4).

Geostatistical analysis through computed mean vector azimuth (MVA) for the studied cross-bedding structures was done by using the standard formula [$MVA = \tan^{-1}(\frac{\sum \sin\theta}{\sum \cos\theta})$] recommended by [32]. Paleocurrent measurements made from different structures may be plotted on a rose diagram for the paleoflow

and source direction of the Wadi Al Qattarah Formation, by using Geo-Rose Program (V. 0.5) graphic software. The geometry of the cross-bedding observed in the study area was classified according to [3].

Table 1: Paleocurrent data of section (1) in the NNW locality.

Formation	Elevation (m)	Facies code	Paleocurrent structure	Dip azimuth	Strike
Wadi Al Qattarah	340 to 343 (~3m thick)	LOPF	Low-angle cross-bedding	100, 99, 100, 101, 101, 98, 101, 99, 101, 100, 99, 102, 101, 102, 350, 351	10, 9, 10, 11, 11, 8, 11, 9, 11, 10, 9, 12, 11, 12, 80, 81
Wadi Al Qattarah	343 to 344 (~1m thick)	LOPF	Low-angle cross-bedding	100, 100, 102, 101, 347, 348, 350, 102, 101, 102, 99, 102, 101, 98, 103, 99, 100, 100	10, 10, 12, 11, 77, 78, 80, 12, 11, 12, 9, 12, 11, 8, 13, 9, 10, 10
Wadi Al Qattarah	344 to 346 (~2m thick)	LOPF	Low-angle cross-bedding	101, 99, 101, 112, 113, 110, 112, 350, 103, 102, 103, 101, 102, 101, 104, 103, 105, 351, 353, 350	11, 9, 11, 22, 23, 20, 22, 80, 13, 12, 13, 11, 12, 11, 14, 13, 15, 81, 83, 80
Wadi Al Qattarah	346 to 349 (~3m thick)	LOGF	Low-angle cross-bedding	92, 94, 91, 93, 91, 92, 91, 91, 94, 93, 91	2, 4, 1, 3, 1, 2, 1, 1, 4, 3, 1
Wadi Al Qattarah	349 to 351 (~2m thick)	TOPF	Trough cross-bedding	107, 106, 107, 107, 109, 108, 106, 107, 109, 101, 110, 101, 108,	17, 16, 17, 17, 19, 18, 16, 17, 19, 11, 20, 11, 18
Wadi Al Qattarah	351 to 356 (~5m thick)	TOGF	Trough cross-bedding	106, 108, 106, 107, 109, 105, 106, 110, 115, 109, 107, 108, 101, 103, 103, 105, 103, 104, 106, 105, 102, 107, 102, 106, 103, 107, 107, 101, 106, 103, 104, 103	16, 18, 16, 17, 19, 15, 16, 20, 25, 19, 17, 18, 11, 13, 13, 15, 13, 14, 16, 15, 12, 17, 12, 16, 13, 17, 17, 11, 16, 13, 14, 13
Wadi Al Qattarah	Above 360 (~3m thick)	LOPF	Low-angle cross-bedding	349, 348, 349, 103, 109, 109, 104, 102, 101, 108, 104, 110, 109, 107, 104, 103	79, 78, 79, 13, 19, 19, 14, 12, 11, 18, 14, 20, 19, 17, 14, 13

Table 2: Paleocurrent data of section (2) in the NNE locality.

Formation	Elevation (m)	Facies code	Paleocurrent structure	Dip azimuth	Strike
Wadi Al Qattarah	361 to 362½ (~1.5m thick)	LOPF	Low-angle cross-bedding	96, 97, 98, 97, 96, 97, 99, 98, 97, 98, 97, 100, 93, 353, 353, 347, 347, 350, 350, 93, 91, 91, 92, 92, 91, 100, 99, 97, 99, 95, 96, 107, 99, 98, 90, 90, 91, 92, 90, 92, 91, 91, 93, 93, 104, 103,	

				102, 105, 109, 101, 99, 100, 100, 103, 101, 99, 101, 101, 98, 100, 101, 99	
Wadi Al Qattarah	Below 363 (~½m thick)	LOGF	Low-angle cross-bedding	98, 100, 98, 98, 98, 97, 98, 98, 99, 97, 99, 98, 99, 97, 99, 100, 101, 103, 110, 109, 109, 103, 104, 104, 99, 100, 98, 100, 101, 99, 102, 100, 105, 101, 102, 99, 101, 101, 99, 98, 97, 103, 101, 97, 98, 101, 98, 99 103, 101, 111, 98, 100, 98, 100, 101, 99, 98, 101, 100, 97, 95, 105, 97, 97, 101, 102, 100, 103, 98, 98, 96, 97	8, 10, 8, 8, 8, 7, 8, 8, 9, 7, 9, 8, 9, 7, 9, 10, 11, 13, 20, 19, 19, 13, 14, 14, 9, 10, 8, 10, 11, 9, 12, 10, 15, 11, 12, 9, 11, 11, 9, 8, 7, 13, 11, 7, 8, 11, 8, 9, 13, 11, 21, 8, 10, 8, 10, 11, 9, 8, 11, 10, 7, 5, 15, 7, 7, 11, 12, 10, 13, 8, 8, 6, 7,
Wadi Al Qattarah	363 to 364 (~1m thick)	TOPF	Trough cross-bedding	109, 109, 110, 109, 115, 111, 108, 110, 109, 103, 115, 111, 110, 111, 107, 104, 103, 103, 110, 102, 101, 101, 101, 109, 109, 102, 103, 105, 105, 105, 110	19, 19, 20, 19, 25, 21, 18, 20, 19, 13, 25, 21, 20, 21, 17, 14, 13, 13, 20, 12, 11, 11, 11, 19, 19, 12, 13, 15, 15, 15, 20
Wadi Al Qattarah	364 to 365 (~1m thick)	TOGF	Trough cross-bedding	103, 104, 105, 105, 102, 103, 101, 103, 112, 113, 111, 112, 112, 112, 115, 107, 107, 109, 105, 102	13, 14, 15, 15, 12, 13, 11, 13, 22, 23, 21, 22, 22, 22, 25, 17, 17, 19, 15, 12
Wadi Al Qattarah	Above 365 (~½m thick)	TOGF	Trough cross-bedding	109, 103, 108, 107, 103, 110, 107, 99, 100, 97, 99, 101, 99, 97, 98, 97, 97, 100, 103, 109, 107, 108, 111, 107, 113, 111, 108, 106, 106	19, 13, 18, 17, 13, 20, 17, 9, 10, 7, 9, 11, 9, 7, 8, 7, 7, 10, 13, 19, 17, 18, 21, 17, 23, 21, 18, 16, 16
Wadi Al Qattarah	Below 366 (~½m thick)	TOGF	Trough cross-bedding	114, 115, 119, 111, 110, 112, 119, 114, 113, 114, 107, 102, 110, 110, 348, 348, 350, 351, 350, 352, 350,	24, 25, 29, 21, 20, 22, 29, 24, 23, 24, 17, 12, 20, 20, 78, 78, 80, 81, 80, 82, 80

Table 3: Paleocurrent data of section (3) in the NE locality.

Formation	Elevation (m)	Facies code	Paleocurrent structure	Dip azimuth	Strike
Wadi Al Qattarah	338 to 339 (~1m thick)	POPF	Planar cross-bedding	109, 110, 110, 109, 110, 101	19, 20, 20, 19, 20, 11
Wadi Al Qattarah	339 to 340 (~1m thick)	TOPF	Trough cross-bedding	109, 109, 110, 109, 108, 108	19, 19, 20, 19, 18, 18
Wadi Al Qattarah	340 to 343½ (~3½m thick)	POGF	Planar cross-bedding	110, 110, 110, 110, 109, 110, 110, 108, 108, 110, 108, 101, 101, 109, 109, 110	20, 20, 20, 20, 19, 20, 20, 18, 18, 20, 18, 11, 11, 19, 19, 20
Wadi Al Qattarah	343½ to 345 (~1½ thick)	TOPF	Trough cross-bedding	104, 108, 102, 101, 103, 102, 108, 103, 107, 107, 101, 101, 101, 103, 109, 108, 108, 103, 108, 103, 102, 108, 102, 108, 101, 103, 108, 108, 107, 108, 109, 112, 111, 109, 110, 111, 101, 108, 108, 101, 108, 111, 109, 108	14, 18, 12, 11, 13, 12, 18, 13, 17, 17, 11, 11, 11, 13, 19, 18, 18, 13, 18, 13, 12, 18, 12, 18, 11, 13, 18, 18, 17, 18, 19, 22, 21, 19, 20, 21, 11, 18, 18, 11, 18, 21, 19, 18
Wadi Al Qattarah	345 to 347½ (~2½m thick)	POPF	Planar cross-bedding	109, 109, 107, 107, 107, 109, 350, 350, 351, 350, 353, 353, 348, 348, 101, 102, 109, 109, 110, 101, 103, 102, 104, 104, 104, 103, 106, 106, 109, 109, 109, 109, 109, 109, 109, 109, 109	19, 19, 17, 17, 17, 19, 80, 80, 81, 80, 83, 83, 78, 78, 11, 12, 19, 19, 20, 11, 13, 12, 14, 14, 14, 13, 16, 16, 19, 19, 19, 19, 19, 19, 19, 19
Wadi Al Qattarah	347½ to 350 (~2½m thick)	LOGF	Low-angle cross-bedding	109, 111, 111, 112, 109, 107, 108, 109, 108, 106, 107, 107, 108, 109, 108, 108, 109, 110, 112, 112, 112, 110	19, 21, 21, 22, 19, 17, 18, 19, 18, 16, 17, 17, 18, 19, 18, 18, 19, 20, 22, 22, 22, 20

Table 4: Paleocurrent data of section (4) in the ENE locality.

Formation	Elevation (m)	Facies code	Paleocurrent structure	Dip azimuth	Strike
Wadi Al Qattarah	337 to 342 (~5m thick)	POPF	Planar cross-bedding	176, 175, 175, 177, 167, 155, 157, 156, 156, 155, 158, 157, 154, 155	86, 85, 85, 87, 77, 65, 67, 66, 66, 65, 68, 67, 64, 65
Wadi Al Qattarah	342 to 348½ (~6½m thick)	LOGF	Low-angle cross-bedding	168, 166, 170, 179, 177, 177, 158, 157, 150, 158, 152, 159, 160, 160, 160, 160, 169, 162, 169, 171, 179, 170, 171, 178, 172, 162, 161,	78, 76, 80, 89, 87, 87, 68, 67, 60, 68, 62, 69, 70, 70, 70, 70, 79, 72, 79, 81, 89, 80, 81, 88, 82, 72, 71,

				168, 169, 160, 160, 169, 169, 169, 166, 169, 169, 169, 167, 170, 178, 163, 168, 169, 159	78, 79, 70, 70, 79, 79, 79, 76, 79, 79, 79, 77, 80, 88, 73, 78, 79, 69
Wadi Al Qattarah	348½ to 350 (~1½m thick)	TOPF	Trough cross-bedding	172, 178, 170, 179, 170, 178, 179, 177, 171, 178, 173, 175, 178, 170, 179, 179, 177, 179, 179, 170, 178, 172, 172	82, 88, 80, 89, 80, 88, 89, 87, 81, 88, 83, 85, 88, 80, 89, 89, 87, 89, 89, 80, 88, 82, 82
Wadi Al Qattarah	350 to 353 (~3m thick)	POPF	Planar cross-bedding	156, 150, 151, 151, 159, 159, 155, 155, 151, 158, 157, 156, 158, 158, 158, 155, 155, 157, 158, 159, 158, 157	66, 60, 61, 61, 69, 69, 65, 65, 61, 68, 67, 66, 68, 68, 68, 65, 65, 67, 68, 69, 68, 67
Wadi Al Qattarah	363½ to 365 (~1½m thick)	HOWF	Herringbone cross-bedding	186, 185, 185, 187, 187, 185, 187, 186, 186, 185, 188, 187, 184, 185, 188, 115, 108, 108, 108, 110, 116, 116, 118, 110, 113, 108, 107, 108, 108, 113, 109, 110, 114, 114, 114, 114, 115, 111, 108, 111, 343, 343, 341, 342, 341, 340, 341, 10, 8, 10, 9, 12, 12, 12, 12	276, 275, 275, 277, 277, 275, 277, 276, 276, 275, 278, 277, 274, 275, 278, 25, 18, 18, 18, 20, 26, 26, 28, 20, 23, 18, 17, 18, 18, 23, 19, 20, 24, 24, 24, 24, 25, 21, 18, 21, 73, 73, 71, 72, 71, 70, 71, 280, 278, 280, 279, 282, 282, 282, 282,

Table 5: Paleocurrent data of section (5) in the SE locality.

Formation	Elevation (m)	Facies code	Paleocurrent structure	Dip azimuth	Strike
Wadi Al Qattarah	363½ to 364½ (~1m thick)	POPF	Planar cross-bedding	177, 178, 170, 167, 169, 160, 167, 170, 166, 165, 179, 179, 179, 169, 163, 168, 161, 155, 152, 179, 179, 161, 172, 172, 172, 170, 169, 177, 159, 158, 158, 158, 158	87, 88, 80, 77, 79, 70, 77, 80, 76, 75, 89, 89, 89, 79, 73, 78, 71, 65, 62, 89, 89, 71, 82, 82, 82, 80, 79, 87, 69, 68, 68, 68, 68
Wadi Al Qattarah	364½ to 365½ (~1m thick)	POGF	Planar cross-bedding	169, 175, 166, 178, 166, 170, 172, 179, 173, 178, 173, 178, 178, 179, 178, 170, 172, 166, 166, 164, 160, 167, 161, 166	79, 85, 76, 88, 76, 80, 82, 89, 83, 88, 83, 88, 88, 89, 88, 80, 82, 76, 76, 74, 70, 77, 71, 76
Wadi Al Qattarah	366½ to 367 (~½m thick)	POGF	Planar cross-bedding	170, 178, 173, 173, 173	80, 88, 83, 83, 83

Table 6: Paleocurrent data of section (6) in the SSE locality.

Formation	Elevation (m)	Facies code	Paleocurrent structure	Dip azimuth	Strike
Wadi Al Qattarah	344 to 347 (~3m thick)	POPF	Planar cross-bedding	150, 151, 147, 149, 149, 152, 152, 149, 151, 148	60, 61, 57, 59, 59, 62, 62, 59, 61, 58
Wadi Al Qattarah	347 to 350 (~2m thick)	LOPF	Low-angle cross-bedding	147, 147, 149, 141, 150, 141, 148, 149, 148, 141, 142, 143, 149, 151, 150, 150, 152, 150, 151, 150, 150, 151, 153, 154, 154	57, 57, 59, 51, 60, 51, 58, 59, 58, 51, 52, 53, 59, 61, 60, 60, 62, 60, 61, 60, 60, 61, 63, 64, 64
Wadi Al Qattarah	350 to 353 (~3m thick)	TOPF	Trough cross-bedding	148, 149, 153, 152, 152, 149, 150, 150, 151, 150, 151, 151, 151, 149, 153, 152, 153, 150, 151	58, 59, 63, 62, 62, 59, 60, 60, 61, 60, 61, 61, 61, 59, 63, 62, 63, 60, 61
Wadi Al Qattarah	353 to 357 (~4m thick)	TOGF	Trough cross-bedding	178, 170, 170, 178, 179, 170, 171, 179, 179, 174, 179, 171, 178, 172, 170, 179, 178, 173, 179, 171, 172, 174, 179	88, 80, 80, 88, 89, 80, 81, 89, 89, 84, 89, 81, 88, 82, 80, 89, 88, 83, 89, 81, 82, 84, 89

Table 7: Paleocurrent data of section (7) in the SSW locality.

Formation	Elevation (m)	Facies code	Paleocurrent structure	Dip azimuth	Strike
Wadi Al Qattarah	339 to 345 (~6m thick)	POPF	Planar cross-bedding	101, 101, 105, 101, 99, 108, 108, 98, 105	11, 11, 15, 11, 9, 18, 18, 8, 15
Wadi Al Qattarah	345 to 353 (~8m thick)	POGF	Planar cross-bedding	109, 101, 109, 101, 101, 106, 109, 110, 100, 100, 107, 107, 104, 104, 104, 104	19, 11, 19, 11, 11, 16, 19, 20, 10, 10, 17, 17, 14, 14, 14, 14
Wadi Al Qattarah	353 to 357 (~4m thick)	TOPF	Trough cross-bedding	108, 103, 101, 110, 100, 109, 98, 100, 99, 99, 98, 97, 343, 347, 344, 344, 110, 108, 111, 109, 109, 98, 100, 98	18, 13, 11, 20, 10, 19, 8, 10, 9, 9, 8, 7, 73, 77, 74, 74, 20, 18, 21, 19, 19, 8, 10, 8
Wadi Al Qattarah	357 to 363 (~6m thick)	TOGF	Trough cross-bedding	100, 103, 105, 100, 101, 108, 110, 108, 101, 100, 100, 109, 110, 111, 111, 107, 108, 106, 106, 104, 106, 109, 107, 114, 106, 352, 354, 350, 98, 99, 98, 100	10, 13, 15, 10, 11, 18, 20, 18, 11, 10, 10, 19, 20, 21, 21, 17, 18, 16, 16, 14, 16, 19, 17, 24, 16, 82, 84, 80, 8, 9, 8, 10

Table 8: Paleocurrent data of section (8) in the WSW locality.

Formation	Elevation (m)	Facies code	Paleocurrent structure	Dip azimuth	Strike
Wadi Al Qattarah	342 to 345 (~3m thick)	TOPF	Trough cross-bedding	99, 109, 107, 109, 105, 101, 101, 101, 110, 101, 103	9, 19, 17, 19, 15, 11, 11, 11, 20, 11, 13
Wadi Al Qattarah	347 to 350 (~3m thick)	POGF	Planar cross-bedding	99, 102, 99, 100, 100, 103, 100, 99, 102, 101, 98, 98, 102	9, 12, 9, 10, 10, 13, 10, 9, 12, 11, 8, 8, 12
Wadi Al Qattarah	350 to 352 (~2m thick)	POPF	Planar cross-bedding	99, 101, 97, 98, 99, 96, 100, 101, 101, 96, 97	9, 11, 7, 8, 9, 6, 10, 11, 11, 6, 7
Wadi Al Qattarah	352 to 355 (~3m thick)	HOWF	Herringbone cross-bedding	188, 189, 183, 182, 182, 189, 180, 180, 181, 180, 181, 181, 181, 189, 183, 182, 183, 180, 110, 110, 110, 113, 109, 107, 114, 106, 112, 112, 112, 112, 112, 109, 113, 108, 108, 272, 270, 271, 273, 272, 285, 285, 285, 9, 9, 10, 9, 10, 8, 8, 9, 9	278, 279, 273, 272, 272, 279, 270, 270, 271, 270, 271, 271, 271, 279, 273, 272, 273, 270, 20, 20, 20, 23, 19, 17, 24, 16, 22, 22, 22, 22, 22, 19, 23, 18, 18, 2, 0, 1, 3, 2, 15, 15, 15, 279, 279, 280, 279, 280, 278, 278, 279, 279

IV. Characterization of Measured Vertical Sections of Wadi Al Aqar Quarry

The Wadi Al Qattarah Formation at Wadi Al Aqar Quarry has been described lithologically in eight different vertical sections which are:

Vertical section (1): it is composed of 2m thick of basinal chalky limestone, grey in color, mudstone texture, hard, rarely fossiliferous, representing Early-Middle Eocene Apollonia Formation, which is part of topped by 10m thick of bioturbated oolitic limestone, white in color, wackestone texture, moderately hard. It is graded to low-angle cross-bedded oolitic limestone of grey to white color, packstone to grainstone texture, medium to hard with a thickness of 9m. Following, it is the trough cross-bedded oolitic limestone of white and grey colors, packstone to grainstone texture, moderately hard to hard, comprising a thickness of 7m. The section was capped by massive and low-angle cross-bedded oolitic limestone of packstone texture with a thickness of 7m (Fig. 6).

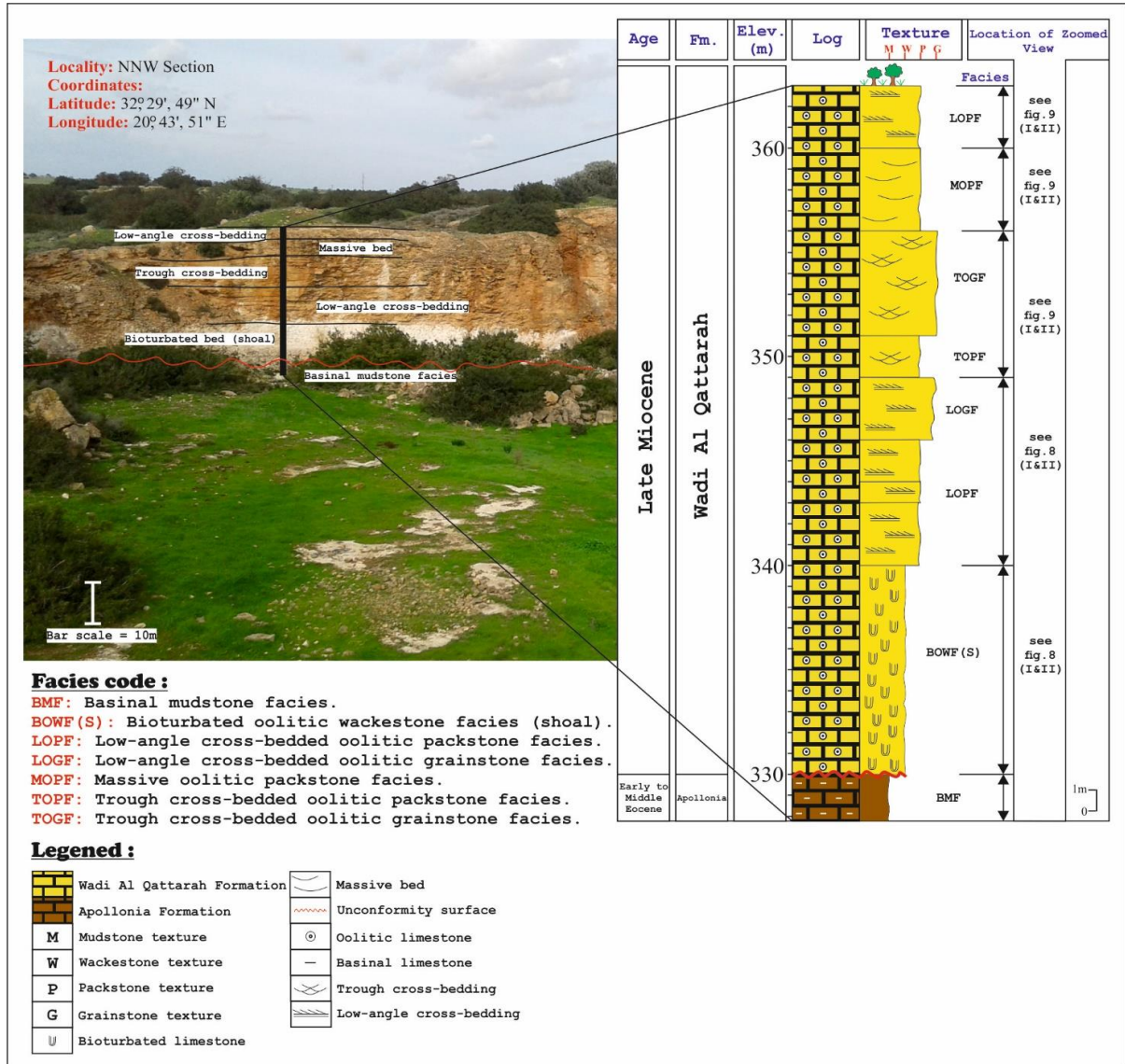


Figure 6 General outcrop view of the vertical section (1) at Wadi Al Aqar Quarry.

Vertical section (2): it is composed of 2m thick low-angle cross-bedded oolitic limestone, grey in color, packstone to grainstone texture, hard. It is graded to channels shoal complex oolitic limestone (trough cross-bedding) of greyish white, packstone to grainstone textures, moderately hard with a thickness of ~2.5m. The section was capped by half meters thick of oolitic packstone facies, grey in color, and moderately soft, (Fig. 7).

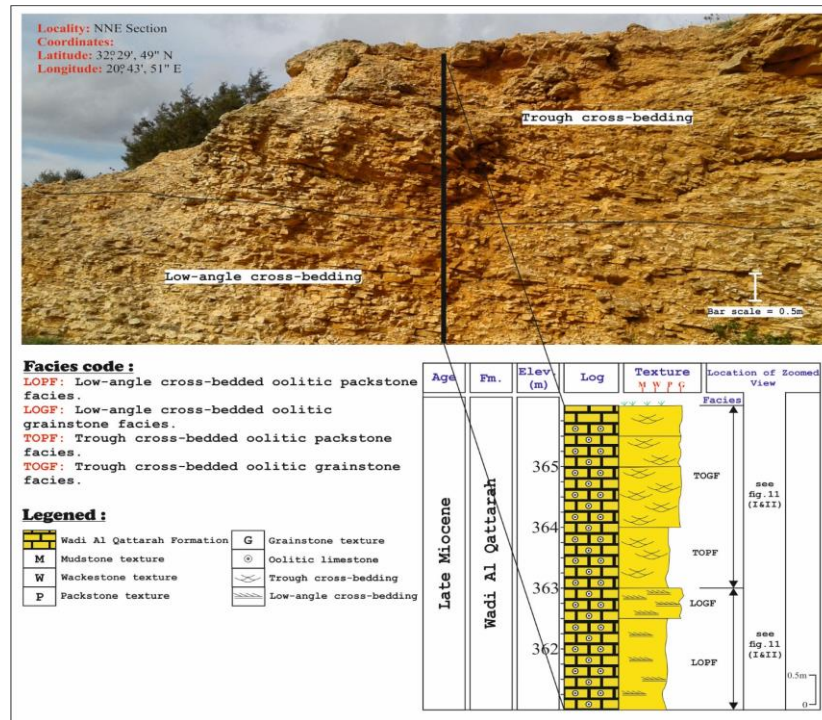


Figure 7 General outcrop view of the vertical section (2) at Wadi Al Aqar Quarry.

Vertical section (3): it is composed of 1m thick of basinal chalky limestone, grey in color, mudstone texture, hard, poorly fossiliferous, representing Early-Middle Eocene Apollonia Formation, which is part of topped by 8m thick of bioturbated oolitic limestone, white in color, wackestone texture, moderately hard. It is graded to planar to trough cross-bedded oolitic limestone of greyish white, packstone to grainstone texture respectively, moderately hard to soft with a thickness of 5.5m. Following, it is the trough and planar cross-bedded oolitic limestones of white in color, packstone texture, and hard, comprising a thickness of 4m. The section was capped by low-angle cross-bedded oolitic limestone of grainstone texture with a thickness of 2.5m to a bioturbated back shoal of wackestone facies (1m thick) (Fig. 8).

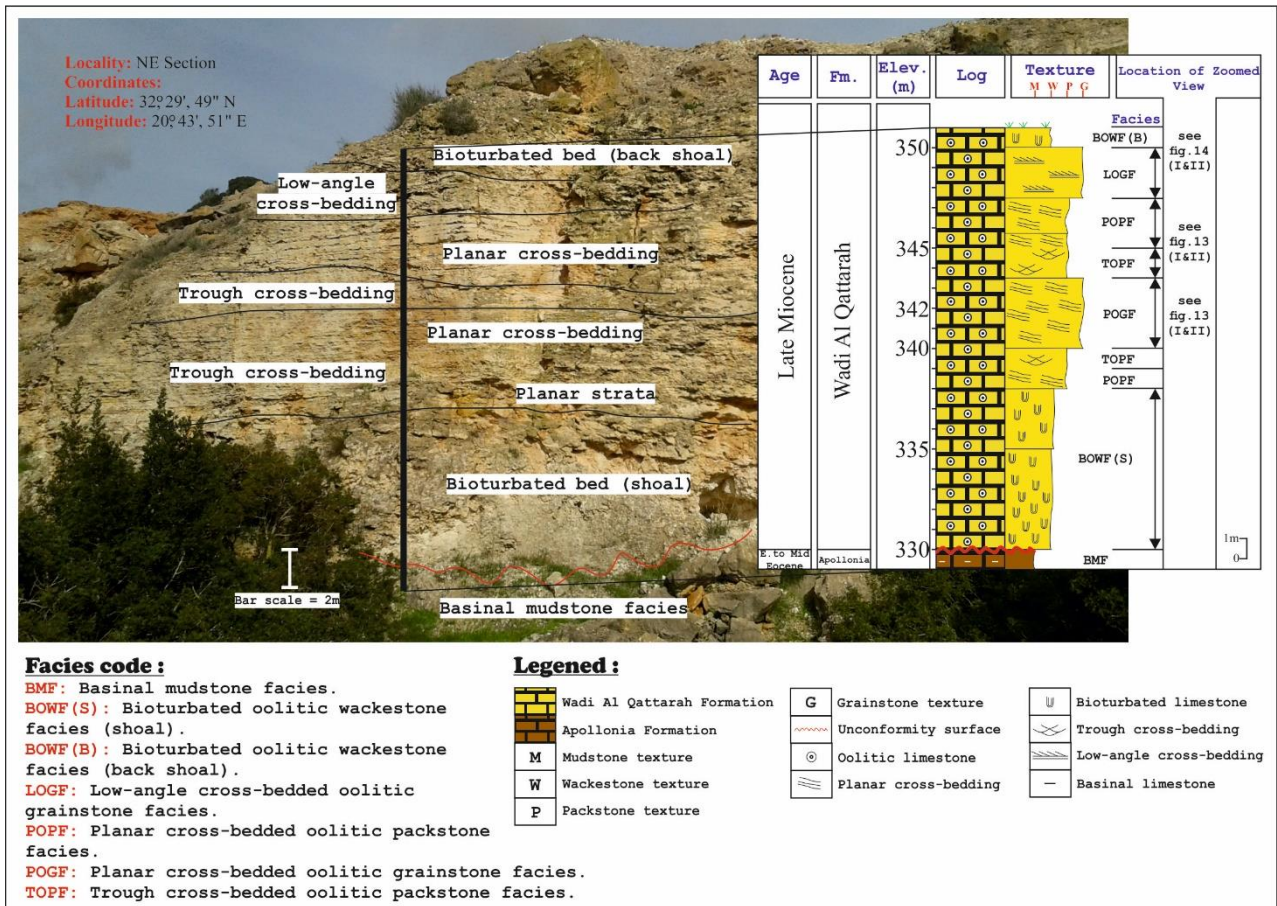


Figure 8 General outcrop view of the vertical section (3) at Wadi Al Aqar Quarry.

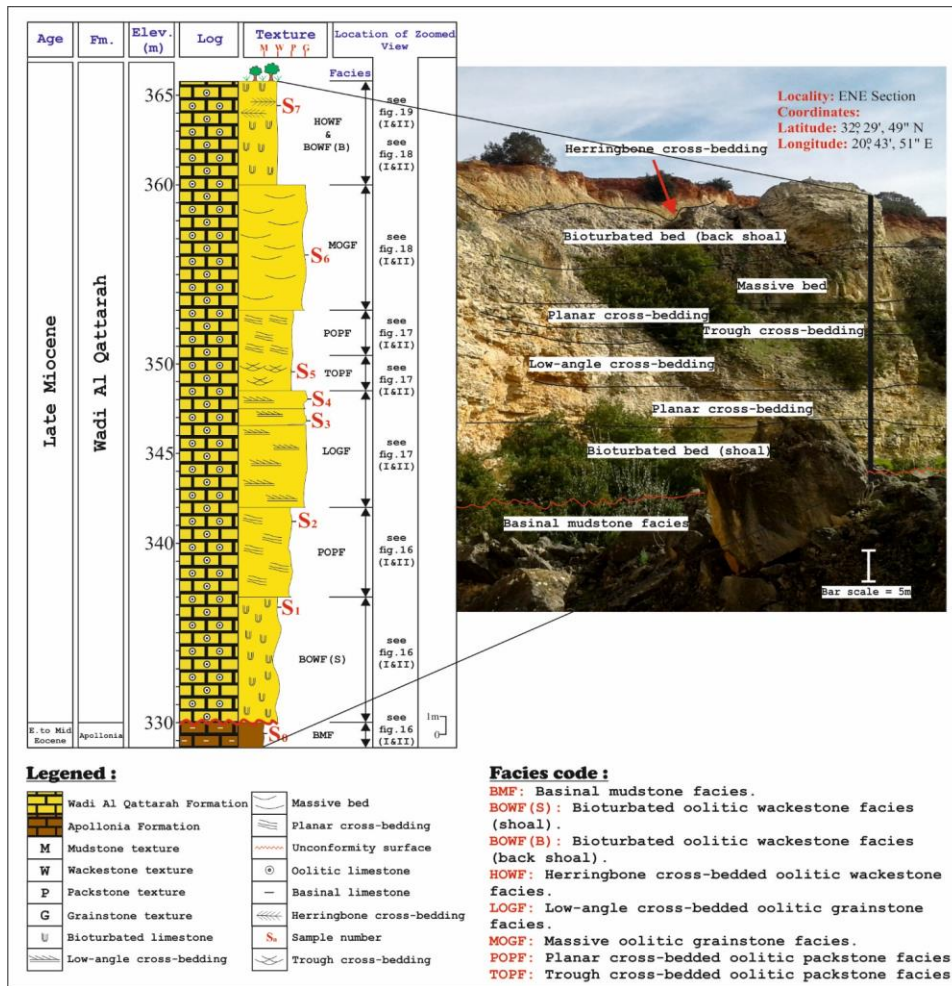


Figure 9 General outcrop view of the vertical section (4) at Wadi Al Aqr

Vertical section (5): it is composed of 0.5m thick of massive oolitic limestone, white to grey, packstone texture, moderately soft, representing Late Miocene Wadi Al Qattarah Formation which is part of topped by 2m thick of planar cross-bedded oolitic limestone, grey in color, packstone to grainstone texture, moderately hard. It is repeated to massive/planar oolitic limestone of grey and white colors, packstone to grainstone texture, moderately soft to hard with a thickness of 1.5m. (Fig. 10).

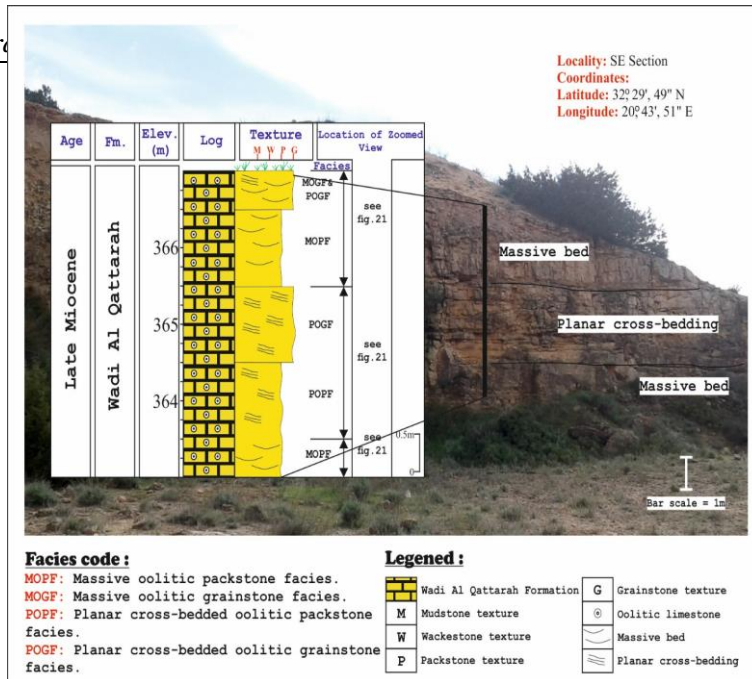


Figure 10 General outcrop view of the vertical section (5) at Wadi Al Aqar Quarry.

Vertical section (6): it is composed of 2m thick of basinal chalky limestone, grey in color, mudstone texture, hard, poorly fossil content representing Early-Middle Eocene Apollonia Formation, which is part of topped by 9m thick of bioturbated oolitic limestone, grey in color, wackestone texture, moderately hard. It is graded to planar\low-angle cross-bedded oolitic limestones of grey and white colors, packstone texture, and moderately soft with a thickness of 6m. Following, it is the trough cross-bedded oolitic limestone of white, packstone to grainstone texture, moderately soft to hard, comprising a thickness of 7m. The section was capped by bioturbated back shoal facies of wackestone texture with a thickness of about 3m (Fig. 11).

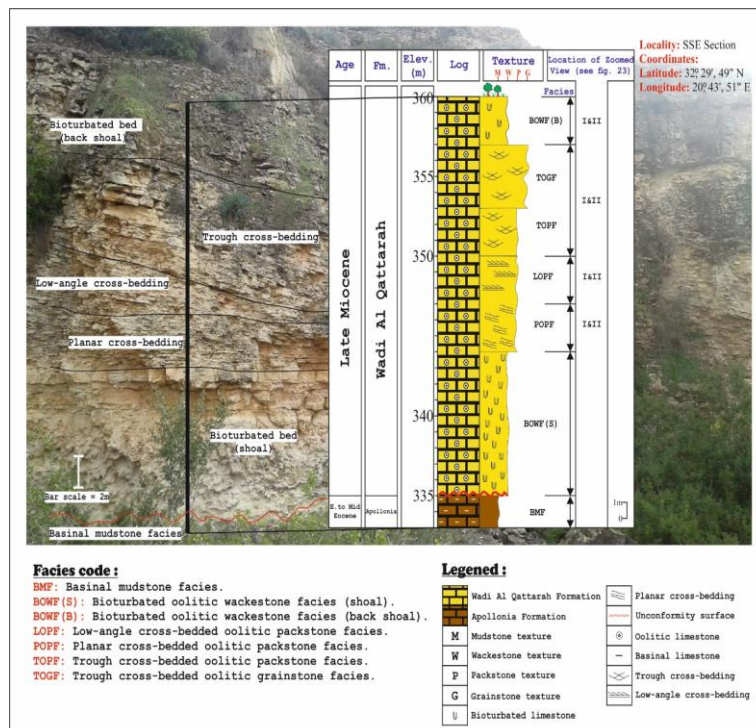


Figure 11 General outcrop view of the vertical section (6) at Wadi Al Aqar Quarry.

Vertical section (7): it is composed of 4m thick of bioturbated oolitic limestone, white in color, wackestone texture, moderately hard, which is part of topped by 14m thick of planar cross-bedded oolitic limestone, white to grey, packstone to grainstone texture, moderately soft. Following, it is the trough cross-bedded oolitic limestone of white, packstone to grainstone texture, hard, comprising a thickness of 10m at the top of the section. (Fig. 12).

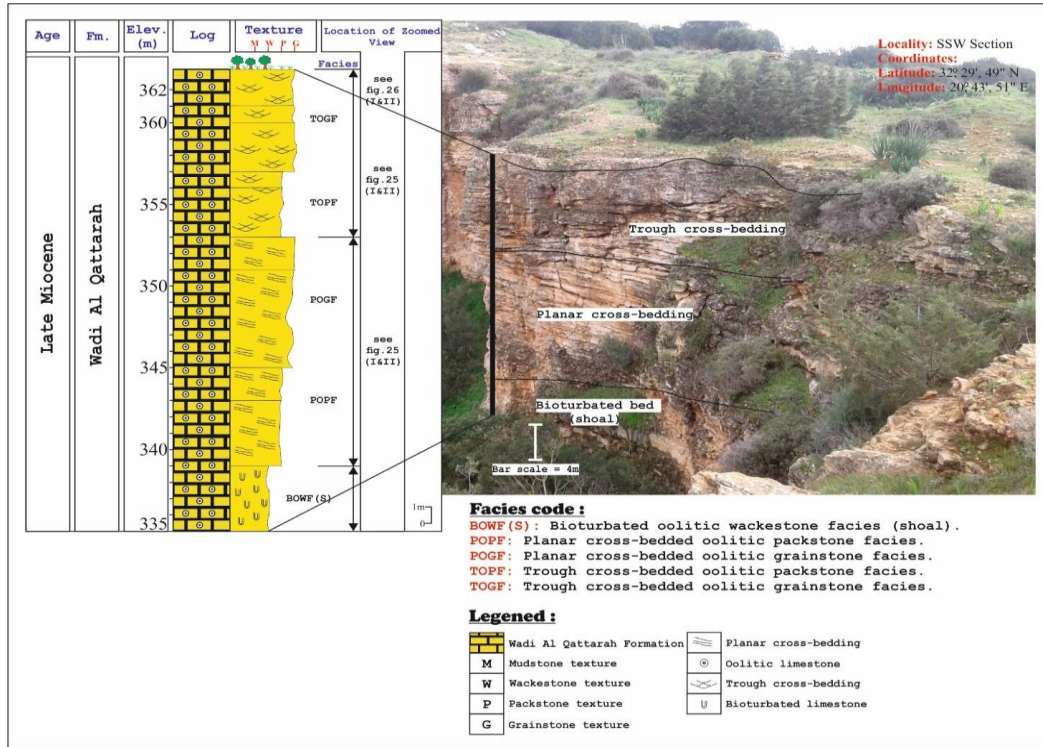


Figure 12 General outcrop view of the vertical section (7) at Wadi Al Aqr Quarry.

Vertical section (8): it is composed of 7m thick bioturbated oolitic limestone, white to grey, wackestone texture, moderately hard, which is part of topped by 5m thick of trough cross-bedded/massive oolitic limestone, grey in color, packstone/grainstone texture, moderately hard to soft. It is graded to planar cross-bedded oolitic limestone of grey to white, grainstone/packstone textures, moderately soft with a thickness of 5m. The section was capped by herringbone cross-bedded oolitic limestone facies of wackestone texture with a thickness of about 3m (Fig. 13).

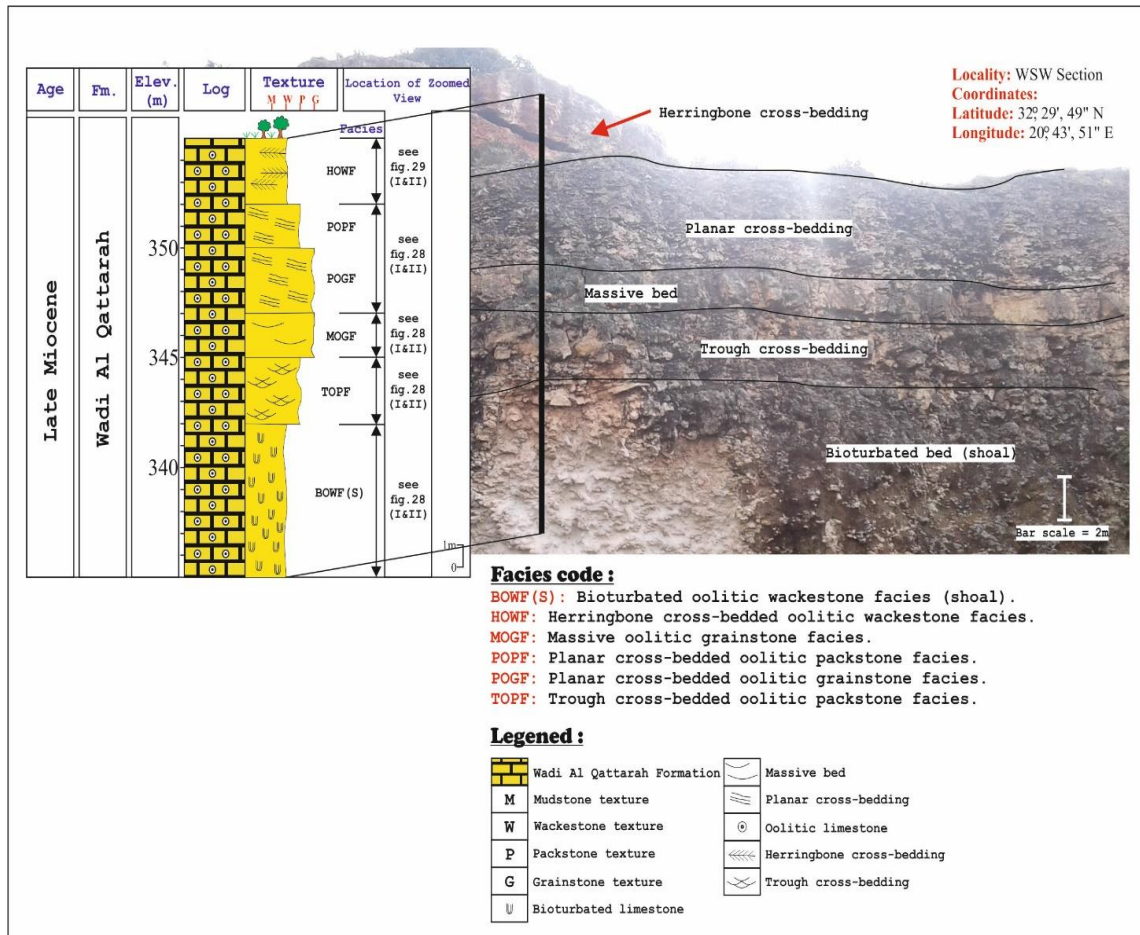


Figure 13 General outcrop view of the vertical section (8) at Wadi Al Aqar Quarry.

V. Geostatistical Analysis and Graphic Presentation of Directional Data

The resultant direction (vector resultant) is usually represented by an arrow at the center of the diagram, and the length of the arrow is proportional to the vector strength. Paleocurrent data may be entered in a field notebook and subsequently published in tabular form (Tables 1 to 8). The azimuths are, however, generally manipulated in some way to make their interpretation easier. The diagram plots lines at every 360 degrees of a compass distribution, with class intervals, are used (10° or 20° or 30°), but a 30° interval will be used in this study. It is better to plot the percentage of observations in each class than to plot the total number of observations.

Geostatistical analysis of cross-bedding attitudes in the study area can easily define these structures and delineate the direction of dip of their axes with the aid of the mean vector azimuth standard method [MVA = $\tan^{-1}(\frac{\sum \sin\theta}{\sum \cos\theta})$] recommended by [32]. Graphic presentation of these measured structures was conducted by using the Geo-Rose Program (V. 0.5) graphic software. By using this program, we easily worked out the data input to produce a worksheet with a defined frequency percentage to be used in the plotting mode to generate a rose diagram.

When all measurements of structures are plotted in the rose diagram, the distribution of paleoflow direction may be seen in a single mode (unimodal) or is different in two or more subequal modes (bimodal or polymodal). In the case of opposite azimuth values, the produced rose could be seen as two reflected values.

All paleoflow measurements from the studied structures may be plotted on a single composite rose diagram which is called a composite rose diagram [33].

Visual observation of the Wadi Al Qattarah Formation in the study area at Wadi Al Aqar Quarry reveals a large range of syndepositional sedimentary structures. These structures are distributed within the measured vertical sections including planar cross-bedded, low-angle cross-bedded, trough cross-bedded, and herringbone cross-bedded oolitic limestone structures.

Measured section (1): It is represented in low-angle cross-bedded and trough cross-bedded oolitic limestone structures.

Azimuth dip directions of these structures were obtained. Out of 126 readings obtained from these structures, 81 readings were taken from low-angle cross-bedding and 45 readings from trough cross-bedding. From the readings, the number and percentage frequency for each 30° class of azimuth was calculated (Fig. 14). The result of the calculation shows the mode in the 90° - 119° class to the ESE (Fig. 14).

The vector azimuths of measured structures in section (1) were as follows: low-angle cross-bedding: 90° and 92° and trough cross-bedding: 105° and 106°. The average vector azimuth for section (1) of the study area is 97° and the average bed thickness of the studied units is approximately 19m

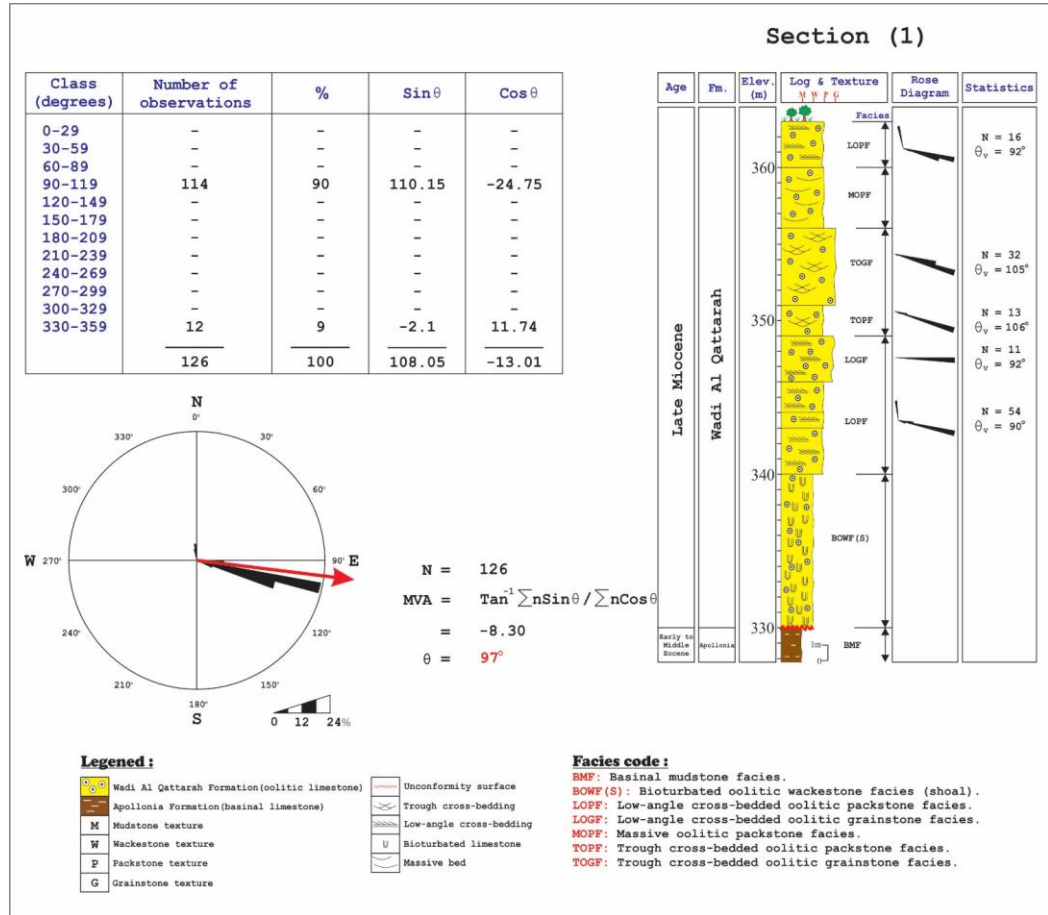


Figure 14 Rose diagram showing frequency distribution of cross beddings azimuths at outcrop level of section (1). Computed statistics is recorded for each studied facies. (N = number of measurements, θ_v = vector mean angle and MVA = mean vector azimuth).

Measured section (2): A total of 239 readings of cross-bedding azimuthal dip directions were taken from this section grouped into two board sedimentary structures: low-angle cross-bedded and trough cross-bedded oolitic limestone structures. 135 readings were taken from low-angle cross-bedding, while 104 readings were taken from trough cross-bedding, respectively.

From there, the number and percentage frequency for each 30° class of azimuth was calculated (Fig. 15). The mode from section (2) is in the 90 - 119° class to the ESE with a minor mode in the 330° - 359° class to the NW (Fig. 15).

The vector azimuths of measured structures in section (2) were as follows: low-angle cross-bedding: 91° and 100° and trough cross-bedding: 98° and 107°. The average vector azimuth for section (2) of the study area is 98°. The bed thickness of the studied units is approximately 4.5m on average.

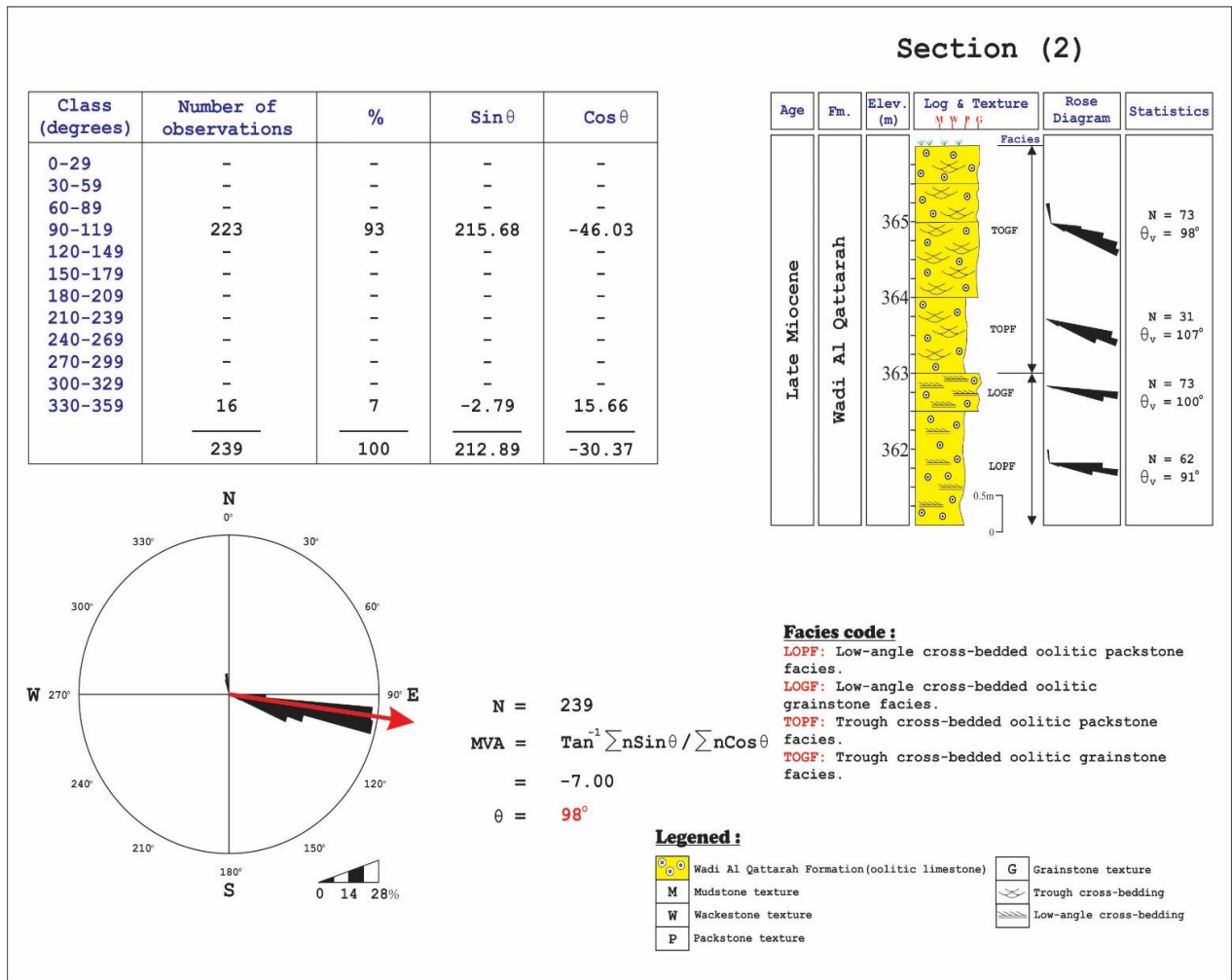


Figure 15 Rose diagram showing frequency distribution of cross beddings azimuths at outcrop level of section (2). Computed statistics is recorded for each studied facies. (N = number of measurements, θ_v = vector mean angle and MVA = mean vector azimuth).

Measured section (3): In the study area, planar cross-bedded, low-angle cross-bedded, and trough cross-bedded oolitic limestone structures were observed in this section. 132 readings of these structures, 60 readings were taken from planar cross-bedding; 22 readings were represented by low-angle cross-bedding, and 50 readings as trough cross-bedding. The class and frequency of azimuths were calculated from the data as shown in figure 16. From the figure, the primary mode is in the 90° - 119° class to the ESE, and the secondary minor mode is in the 330° - 359° class to the NW. The average vector azimuth for section (3) of the study area is 103° and the average bed thickness of the studied units is approximately 11m (Fig. 16).

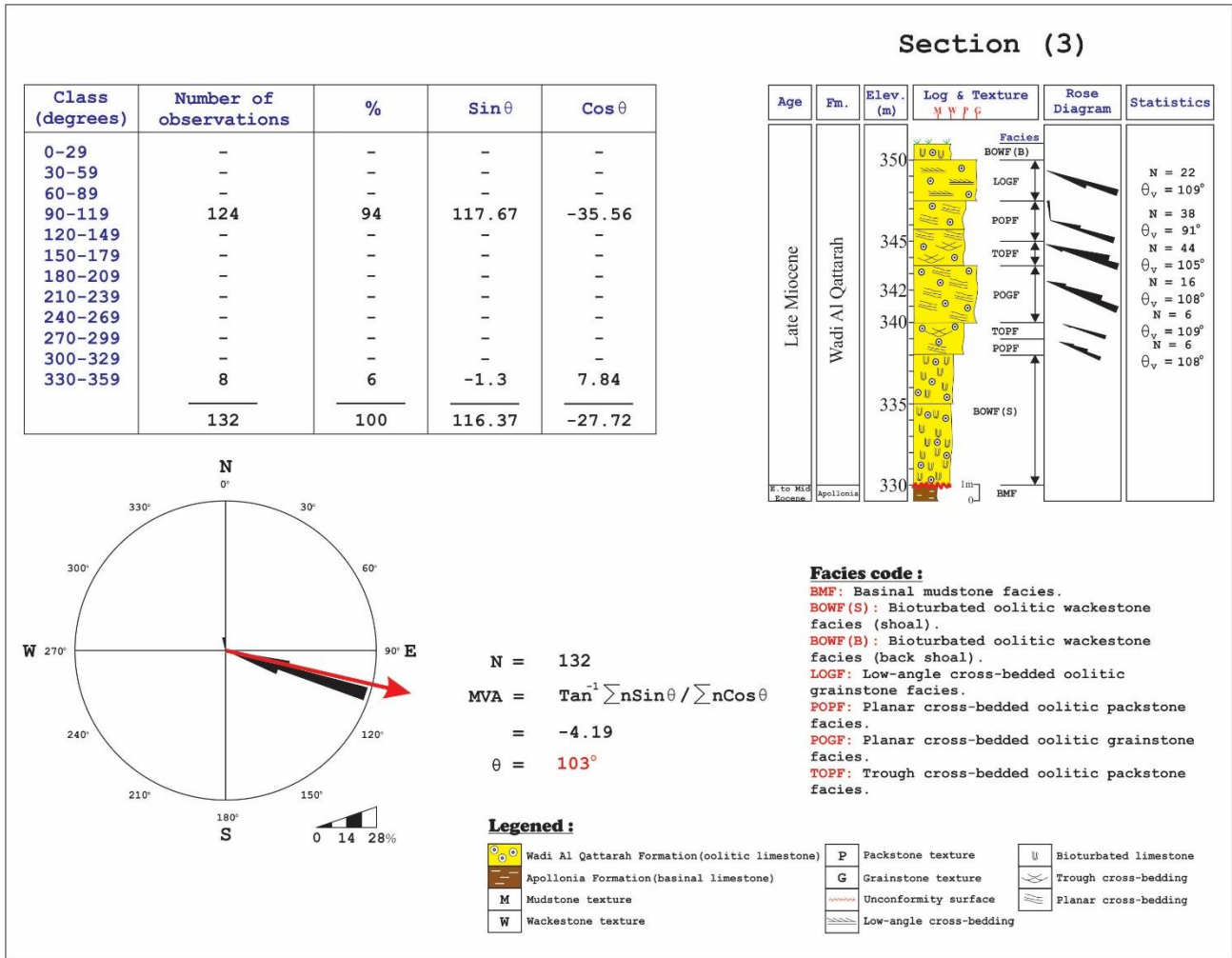


Figure 16 Rose diagram showing frequency distribution of cross beddings azimuths at outcrop level of section (3). Computed statistics is recorded for each studied facies. (N = number of measurements, θ_v = vector mean angle and MVA = mean vector azimuth).

Measured section (4): Most of the sedimentary structures (Fig. 17) were observed in this section of the study area. These structures are planar cross-bedded, low-angle cross-bedded, trough cross-bedded, and herringbone cross-bedded oolitic limestones. 159 readings were taken from this section. From these readings, the primary modal direction in the 150° - 179° class to the SSE, a secondary modal direction in the 330° - 359° class to the NW, and 0° - 29° class to the NE. The average vector azimuth for section (4) of the study area is 157° and the average bed thickness of the studied units is approximately 17.5m.

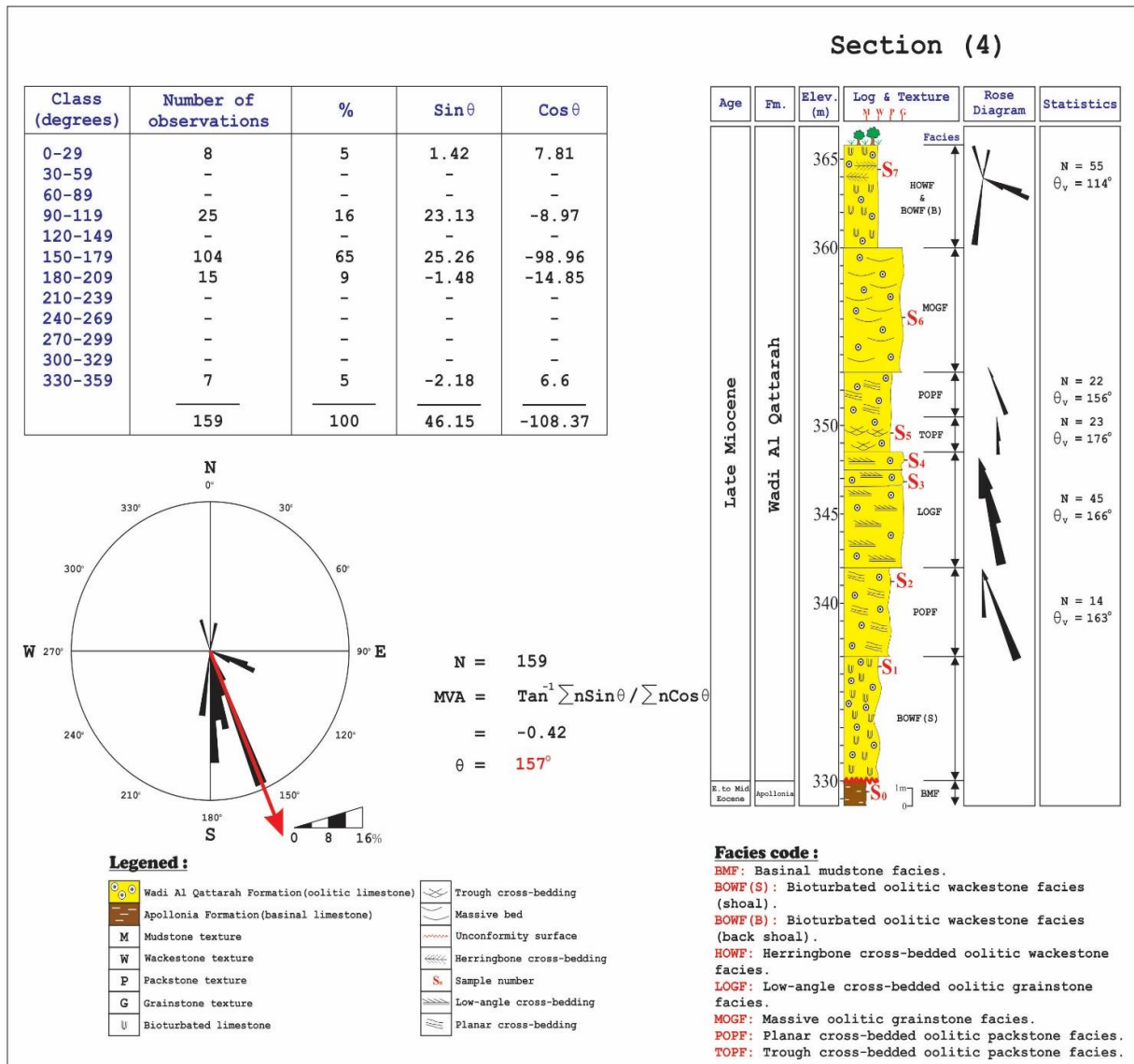


Figure 17 Rose diagram showing frequency distribution of cross beddings azimuths at outcrop level of section (4). Computed statistics is recorded for each studied facies. (N = number of measurements, θ_v = vector mean angle and MVA = mean vector azimuth).

Measured section (5): Only planar cross-bedded oolitic limestone structures were studied in this section. Azimuth dip directions of these structures were measured. Out of 62 readings obtained from these structures. From the readings, the number and percentage frequency for each 30° class of azimuth was calculated (Fig. 18). The result of the calculation shows the mode in the 150° - 179° class to the SSE. The vector azimuth of measured structures in section (5) is 169° and the average bed thickness of the studied units is approximately 2.5m.

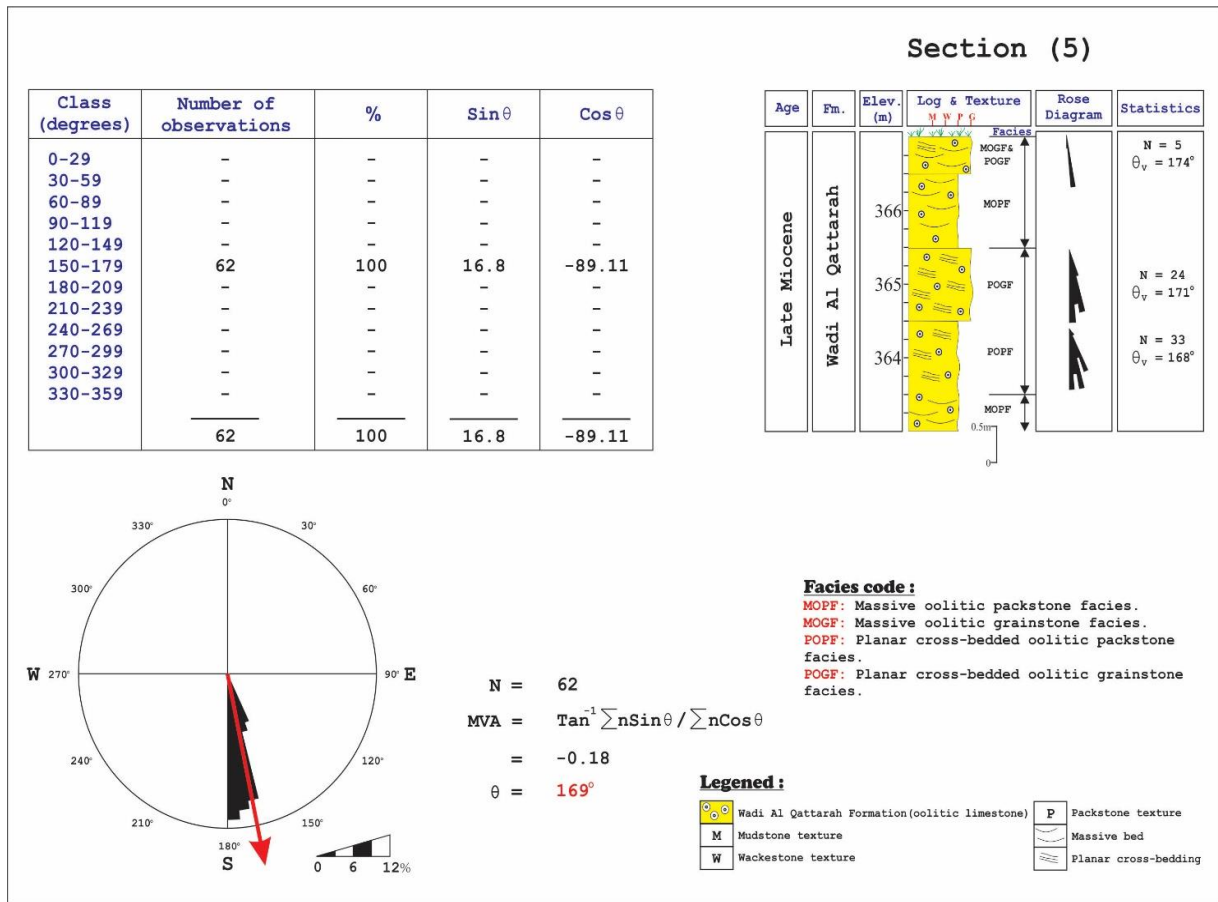


Figure 18 Rose diagram showing frequency distribution of cross beddings azimuths at outcrop level of section (5). Computed statistics is recorded for each studied facies. (N = number of measurements, θ_v = vector mean angle and MVA = mean vector azimuth).

Measured section (6): This section is characterized by planar cross-bedded, low-angle cross-bedded, and trough cross-bedded oolitic limestone structures on the top. 77 readings of structures were calculated and graphically presented as in the rose diagram (Fig.19). This measurement shows that structure direction is modal in 150° - 179° class direction (SSE). The vector azimuth of measured structures and the average bed thickness of section (6) is presented in Figure 19.

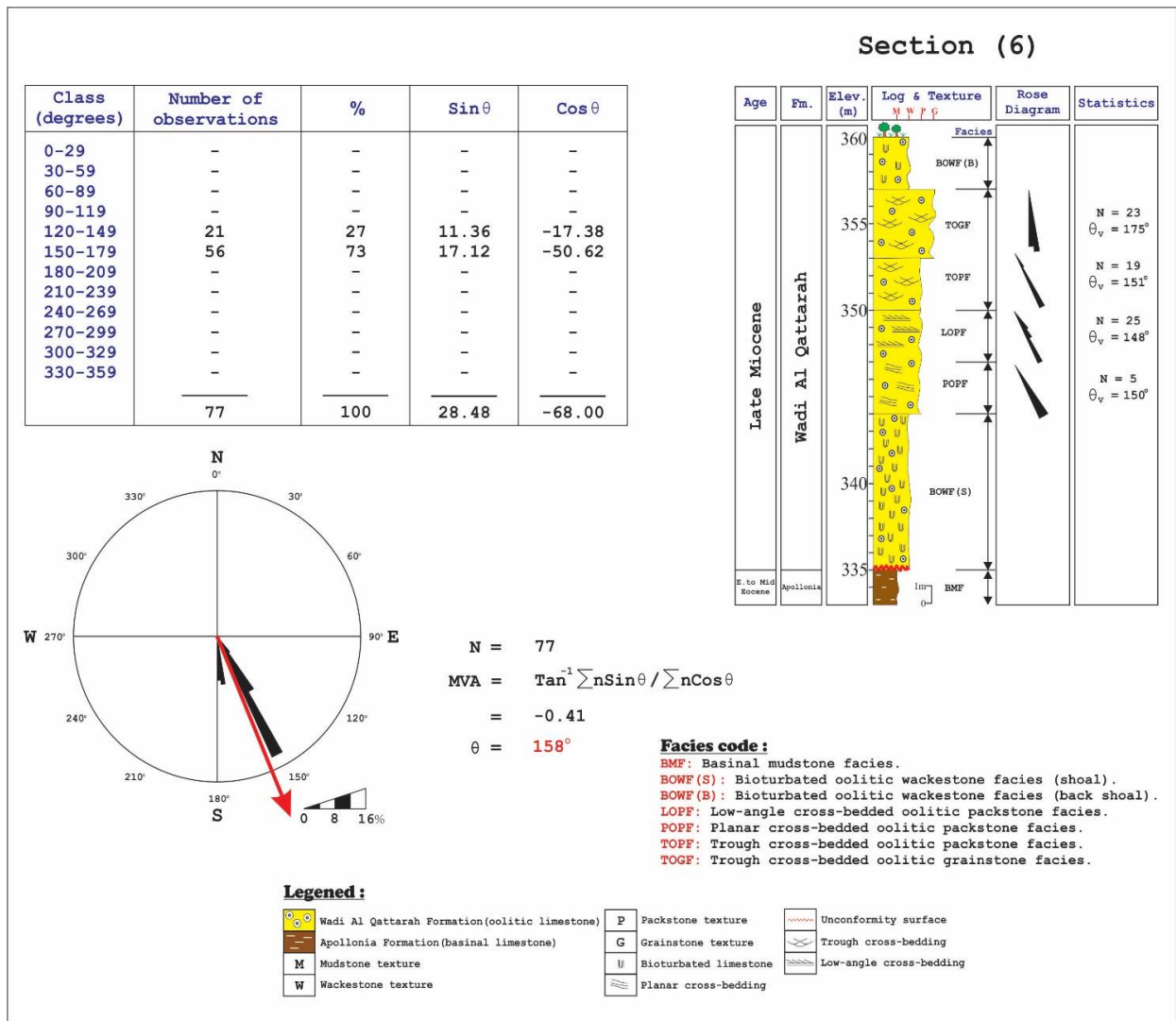


Figure 19 Rose diagram showing frequency distribution of cross beddings azimuths at outcrop level of section (6). Computed statistics is recorded for each studied facies. (N = number of measurements, θ_v = vector mean angle and MVA = mean vector azimuth).

Measured section (7): A total of 81 readings of planar cross-bedded and trough cross-bedded oolitic limestone structures were measured from this section. 25 readings were taken from planar cross-bedding, while 56 readings were taken from trough cross-bedding, respectively. From there, the mode from section (7) is in the 90° - 119° class to the ESE and in the 330° - 359° class to the NW (Fig. 20). The vector azimuths of measured structures in section (7) were as follows: planar strata: 103° and 105° and trough cross-bedding: 92° and 99°. The average vector azimuth for section (7) of the study area is 99° with the bed thickness of the studied units being approximately 24m on average.

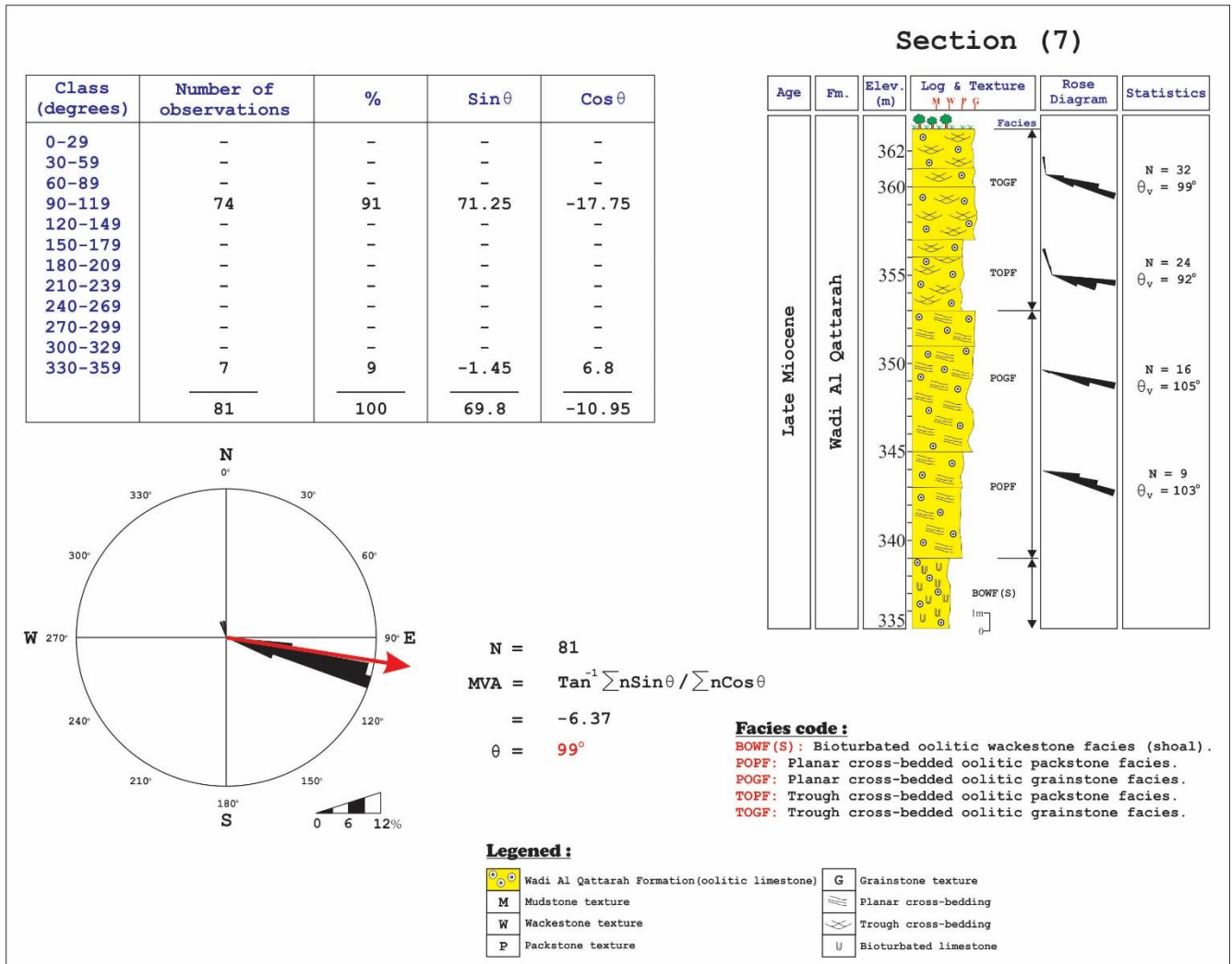


Figure 20 Rose diagram showing frequency distribution of cross beddings azimuths at outcrop level of section (7). Computed statistics is recorded for each studied facies. (N = number of measurements, θ_v = vector mean angle and MVA = mean vector azimuth).

Measured section (8): Some structures were recorded in section 8 in the field. These structures include planar cross-bedded, trough cross-bedded, and herringbone cross-bedded (upper part) oolitic limestones. 24 readings were taken from planar cross-bedded, 11 readings were taken from trough cross-bedding, and 52 readings from herringbone cross-bedding. The class of azimuths (primary mode 90° - 119° class to the ESE and minor secondary modes 180° - 209° class to the SSW, 270° - 299° class to the NW and 0° - 29° class to the NE), number of frequency and percentage frequency were calculated from their azimuths, and the results were summarized and graphically presented as in rose diagram (Fig. 21).

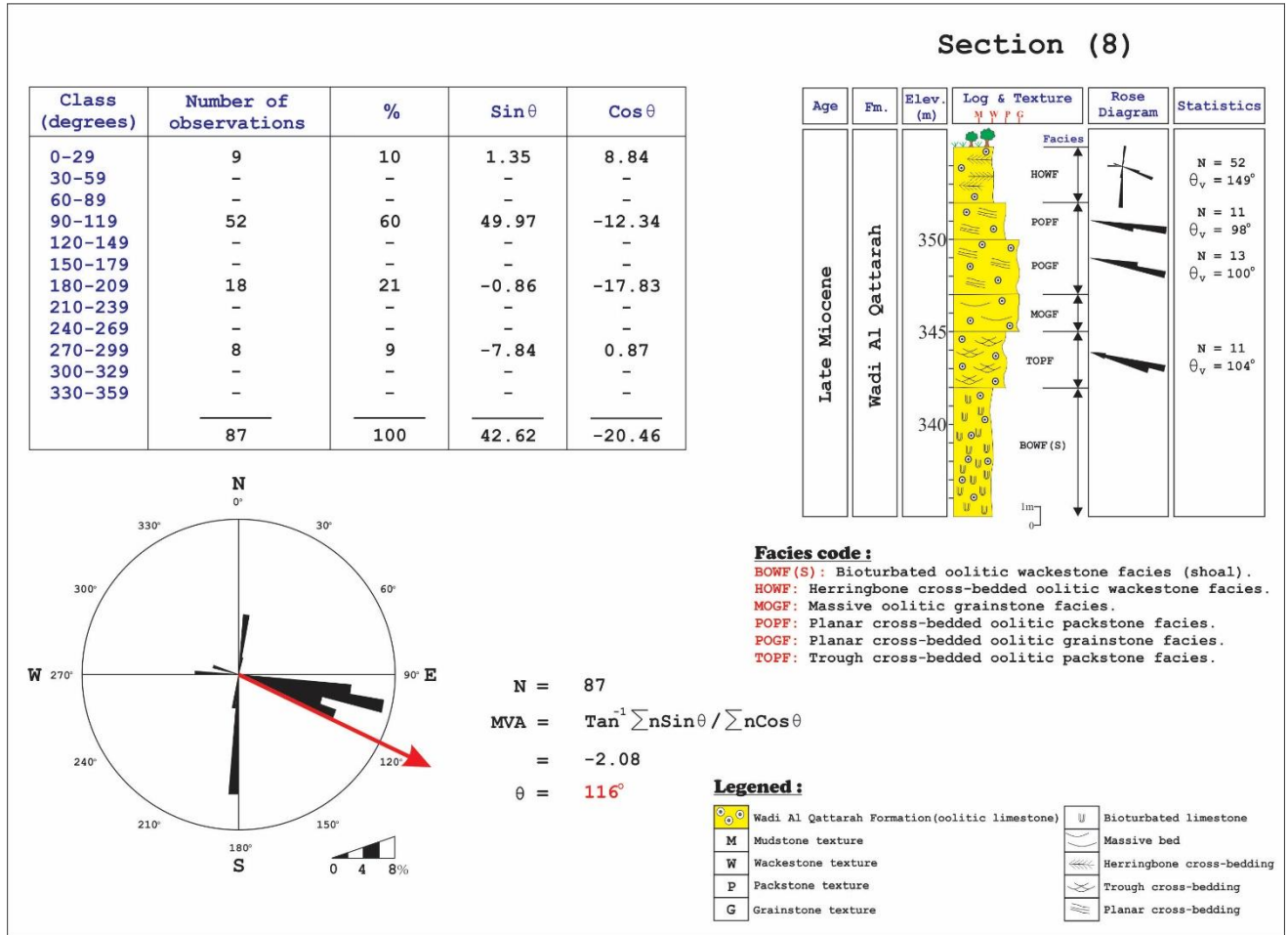


Figure 21 Rose diagram showing frequency distribution of cross beddings azimuths at outcrop level of section (8). Computed statistics is recorded for each studied facies. (N = number of measurements, θ_v = vector mean angle and MVA = mean vector azimuth).

VI. Results and Interpretation

6.1 Results

The regional pattern of directions of cross-beddings in the Wadi Al Qattarah Formation in Wadi Al Aqar Quarry is shown in figures 14 to 21 in which computed statistics are recorded for each studied facies, and the rose diagram shows the frequency distribution and modes for all measurements from each studied facies. Bold arrows represent vector resultants for measurements at a given locality; several striking characteristics of the directions of cross-bedding are evident. In each facies, the principal modes range between 95° and 190° and secondary modes between 275° and 8°.

The primary and secondary modes are, therefore, nearly 178-180 degrees apart. The framework of primary sedimentary structures in each oolitic limestone facies is essentially the same, even though the formation is distributed throughout a thickness of 36m and represents 7 depositional facies.

In general, cross-bedding is asymmetrically distributed about the mode, and around sections (4 and 8) there appears to be considerable scatter. There are slightly some sets in sections (4) and (8) dipping to the southwest, and some others dipping to the northwest and northeast. Therefore, a strongly unidirectional preferred dip to the southeast is obvious in nearly every studied section with only minor reversals to the northwest and northeast observed (Fig. 22).

6.2 Interpretation

Major aspects of the depositional environment of the cross-bedded oolitic and skeletal limestones of the Wadi Al Qattarah Formation can be interpreted with considerable confidence. Under the tectonic setting in which Late Miocene sediments of the Al Jabal Al Akhdar were deposited, rocks of this nature could not

represent an environment other than a shallow marine in which oolitic and skeletal debris was washed back and forth on a shoal. The scale of the cross-bedding, together with associated wackestone deposits and occasional coarse-grained fossil fragments, indicates that the transporting currents were marine.

Cross-bedding directions in the oolitic limestone of the Wadi Al Qattarah Formation indicate that the paleoslope in the Wadi Al Aqar Quarry was to the southeast, during the deposition of the Wadi Al Qattarah Formation. This trend seemingly existed throughout most of the studied facies of the Wadi Al Qattarah Formation. In some facies of the studied sequence, there is strong evidence of highlands in some parts of the quarry as indicated by the minor northwestern and northeastern secondary mode paleocurrent directions in the vicinity of sections 1, 2, 3, 4, 7, and 8 (Fig. 22). Throughout most of the studied Wadi Al Aqar Quarry, however, a strong southeastern paleoslope existed.

The paleogeographic map (Fig. 23) was constructed on a resultant rose diagram which can be defined by (1) oolitic and skeletal debris ridges in the limestone of Wadi Al Qattarah Formation oriented parallel to the direction of 125° mean vector azimuth of the inferred marine paleocurrent, and changing progressively to lagoonal setting in the northwestern and northeastern directions, and (2) ancient shorelines formed arc-shaped with regional NE trends, moved back and forth oriented perpendicular to the marine paleocurrent, where transgression and regression would cause these shorelines to shift through time.

Within these oolitic limestone ridges, most cross-bedding dips seaward (southeast direction) because the ebb tide is stronger. This pattern of the framework is characteristic of the offshore tidal current environment, which may suggest that tidal currents may be a major factor in the dispersal of oolitic and skeletal limestones of the Wadi Al Qattarah Formation.

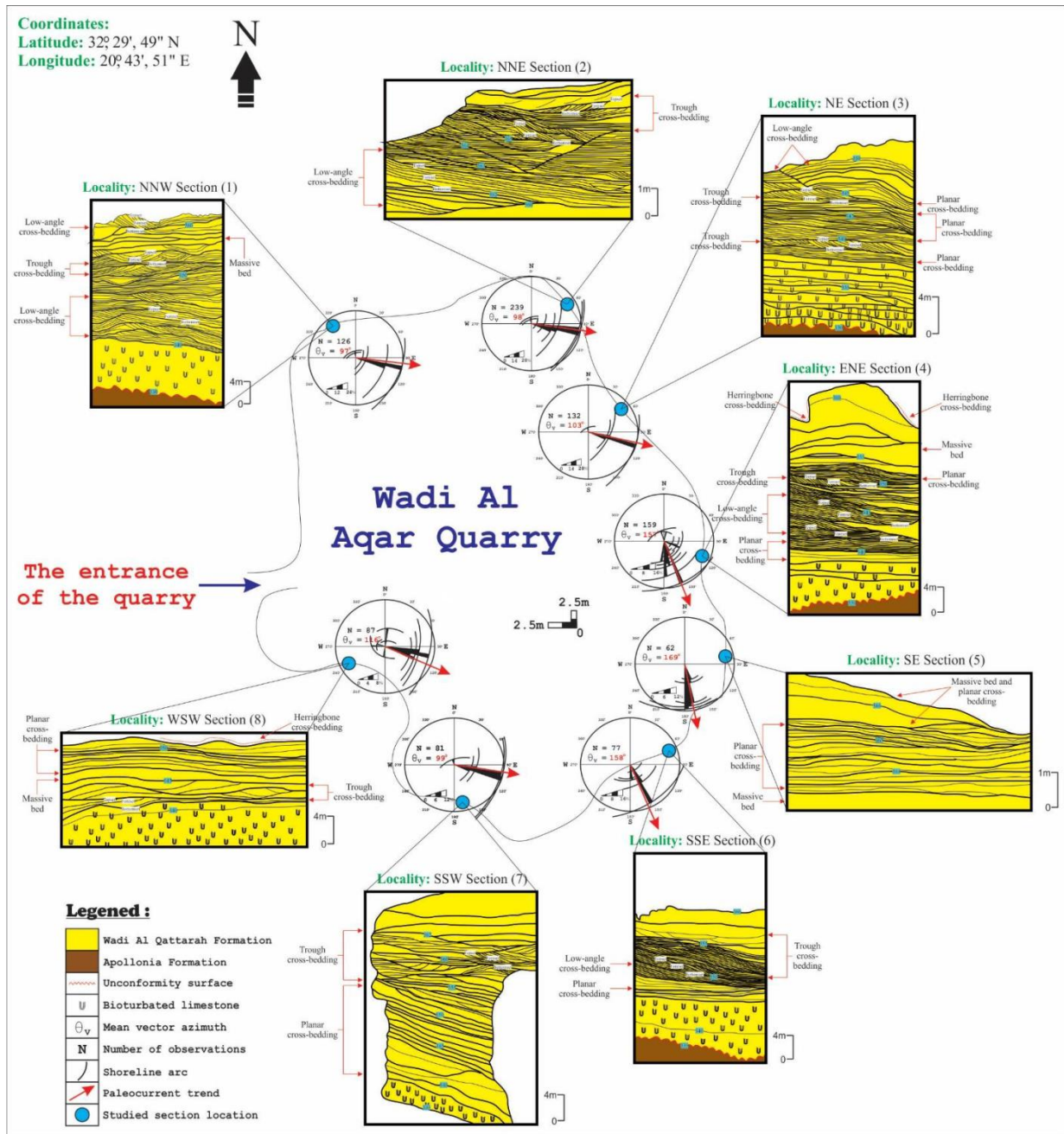


Figure 22 Map showing directions of cross-bedding in the oolitic limestone exposed in Wadi Al Aqar Quarry, NE Libya. Nine hundred and sixty-three (963) measurements were taken in eight sections (Secs. 1-8) at different localities. Note strong primary mode of the resultant vector means to the southeast expressed in summary rose diagrams. Also arc shapes of possible shifted shorelines can also be seen.

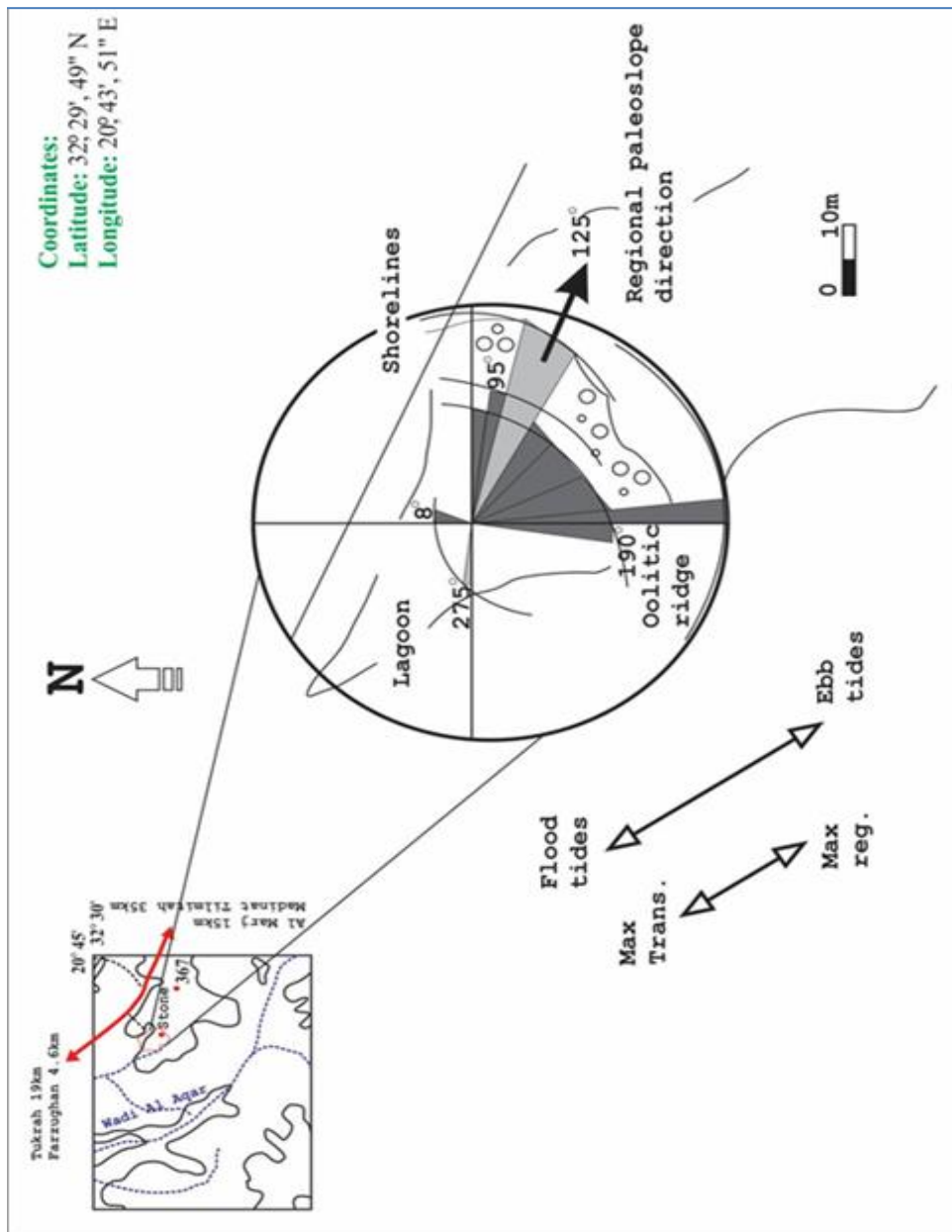


Figure 23 Paleogeographic map showing regional paleoslope, hypothetical trend of shorelines and marine tidal current systems during Wadi Al Qattarah Formation depositional time in Wadi Al Aqar Quarry, NE Libya.

VII. Conclusions

Geostatistical analysis and graphic presentation of cross-bedding directions in the oolitic limestone of Wadi Al Qattarah Formation in Wadi Al Aqar Quarry have revealed that these sedimentary structures are characterized by the primary mode of regional slope dips seaward in the southeast direction, and the secondary minor mode is in northwestern and northeastern directions, indicating a current system moving toward the shore.

Transgression and regression of paleomarine currents would cause ancient shorelines which oriented perpendicular to the marine paleocurrents to shift through time.

The framework of these paleomarine currents has suggested the inferred paleogeography of the Wadi Al Qattarah Formation in Wadi Al Aqar Quarry, in which the dispersal of the oolitic and skeletal limestone ridges in the southeast direction (ebb tide direction), changing to lagoonal settings in the northwestern and northeastern directions (flood tide direction).

Acknowledgments

We would like to express our sincere thanks and appreciation to the Department of Earth Sciences, Faculty of Science at the University of Benghazi for their encouragement to publish this paper. All thanks and appreciation to everyone who contributed with us in facilitating access to the study area and collecting information and samples to prepare this paper.

Deep thanks are also extended to anonymous reviewers for their constructive comments and thoughtful discussions on this paper.

References

- [1]. Boggs, S. (1995) Principles of Sedimentology and Stratigraphy. 2nd Edition, Prentice Hall, New Jersey, 765 p.
- [2]. Potter, P.E., and Pettijohn, F.J. 1978, Paleocurrent and basin Analysis, Academic Press, New York, pp. 296.
- [3]. Boggs, S. Jr. 2006, Principles of sedimentology and stratigraphy, 4th ed., Prentice-Hall, Upper Saddle River, NJ.
- [4]. Klen, I. 1974, Geological map of Libya; 1:250 000 sheet: NI 34-14, Benghazi explanatory booklet, Industrial Research Centre, Tripoli, pp. 49.
- [5]. Francis, M. and Issawi, B. 1977, Geologic map of Libya; 1: 250,000 sheet: Soluq NH 34-2, explanatory booklet, Industrial Research Centre, Tripoli, pp. 86.
- [6]. Mazhar, A. and Issawi, B. 1977, Geologic map of Libya; 1: 250,000 sheet: Zt. Msus NH 34-3. explanatory booklet. Industrial Research Centre, Tripoli, pp. 80.
- [7]. Swedan, A. and Issawi, B. 1977, Sheet Bir Hacheim (NH 34-4), Geological map of Libya, scale 1:250,000, explanatory booklet, Industrial Research Centre, Tripoli.
- [8]. El-Hawat, A.S. and Salem, M.J. 1987, A case study of the stratigraphic subdivision of Ar Rajmah Formation and its implications on the Miocene of northern Libya: In proceedings VIIIth Cong. Med. Neogene Strat., Budapest. Ann. Inst. Geol. Hungary, vol. 70, p. 173-184.
- [9]. El Hawat, A.S. 1986a, Fine-grained current drift carbonates and associated facies in a slope to shelf shoaling-up sequences; the Eocene, NE Libya: In the 7th European I.A.S. Mtg. Ext. Abs. Krakow, Poland, p. 208-210.
- [10]. El Hawat, A.S. 1986b, Large-scale cross-bedded fine-grained contourites and associated facies; A model from the Eocene of NE Libya: 12th. I.A.S. Congress (Abs.). Canberra, Australia, pp. 94.
- [11]. El Hawat, A.S. Abdel Gawad, G.I. and Salem, M.J. 1993, Neogene carbonate discontinuity surfaces in northern Libya. Sedimentary basins of Libya, Geology of Sirt Basin Symp. Abs., Earth Sci. Soci. Libya, Tripoli. pp. 18.
- [12]. Abdulsamad, E. and Barbieri, R. 1999, Foraminiferal distribution and paleoecological interpretation of the Eocene-Miocene carbonates at Jabal Al Akhdar (northeast Libya): Journal of micropaleontology, 18, p. 45-65.
- [13]. Abdulsamad, E.O. Bu Argoub, F.M. and Tmalla, A.F.A. 2009, Stratigraphic review of the Eocene to Miocene rock units in the al Jabal Al Akhdar, NE Libya: Marine and Jour. Petro. Rese. p. 12-35.
- [14]. Abdulsamad, E.O. and El Zanati, S.M. 2013, Miocene benthic foraminifera from the Soluq area, NE Libya: biostratigraphy and environmental significance: Journal of Mediterranean Earth Sciences, v. 5, p. 245-256.
- [15]. Abdulsamad, E.O. and Tmalla, A.F.A. 2013, Systematic paleontology of Oligocene- Miocene planktonic foraminifera from NE Libya. Egypt. Jour. Paleontol., Vol. 13,2013, p. 1-28 ISSN 1687-4986.
- [16]. Amrouni, K.S. Pope, M.C. and Ahmed, S. 2013, Sedimentology and sequence stratigraphy of the Middle to Late Miocene, Al-Jabal Al-Khdar uplift and Soluq Trough, Cyrenaican NE Libya: AAPG 2013 Annual Convention and Exhibition, Pittsburgh, Pennsylvania, May 19-22, p. 4.
- [17]. Amrouni, K.S., and Pope, M.C. 2015, Sequence stratigraphy, chemostratigraphy and diagenesis of the Cyrenaica Miocene carbonate-evaporites successions, NE Libya: Gulf Coast Association of Geological Societies Transactions, <http://www.gcagshouston.com/student-poster-sessions/>, v. 65, p. 21-30.
- [18]. Muftah, A.M. Al-Faitouri, M.S. and El-Ekhfifi, S.S. 2015, Utilization of the observed geological features in differentiating the exposed rock units in Al Jabal Al Akhdar, Libya: First international conference in basic science and their applications, Al Bayda, Libya, 2015. Proceeding book, p. 171-178.
- [19]. Abdulsamad, E.O. El-Ekhfifi, S.S. and Muftah, A.M. 2018, Stratigraphy and larger benthic foraminifera of Middle Eocene to Middle Miocene rocks along the Tobruk-Al Bardia scarps, northeastern Cyrenaica, Libya: Stratigraphy, vol. 15, no. 3, text figures 1-12, plates 1-5, appendix 1, p. 153-178.
- [20]. Elfighi, O. B., El Qumati, A.E., Abdulrahman, F. Al hadad, A. Bukhamada, A. and Gneiber, O. 2018, Lithostratigraphic correlation of the Middle Eocene-Upper Miocene rocks between sectors (1-5), Tansulukh region, Al Jabal Al Akhdar NE Libya: An integrating study from previously studied wadies: Libyan Journal of Science and Technology, 7:1, p. 21-23.
- [21]. Rao, J.S. and Sengupta, S. 1970, Mathematical techniques for paleocurrent analysis: Treatment of directional data: An optimum hierarchical sampling procedure for cross bedding data: Jour. geology, v. 78, no. 5, p. 533-544.
- [22]. Shah, S.M.A. Amer Hafeez, A. and Ahmad, N. 2009, Paleocurrent analysis of Dhok Pathan Formation, from Thathi northeastern Potwar Dist. Rawalpindi: Geol. Bull. Punjab Univ. 44, p. 123-129.
- [23]. Parks, J.M. 1970, Paleocurrent analysis of sedimentary crossbed data with graphic output using three integrated computer programs: Journal of the International Association for mathematical geology volume 6, p. 353-362.
- [24]. Tucker, M.E. 2003, Sedimentary rocks in the field, 3rd ed.: The geological field guide series, pp. 234.
- [25]. Selley, R.C. 2000, Applied sedimentology book, 2nd ed.: Academic Press, San Diego, San Francisco, New York, London, Sydney, Tokyo and Boston, pp. 523.
- [26]. Tucker, M.E. 2011, Sedimentary rocks in the field, 4th ed.: A practical field guide, pp. 288.
- [27]. El-Hawat, A.S. and Abdulsamad, E.O. 2004, The geology of Cyrenaica: A field seminar. Earth Sciences Society of Libya (ESSL), Special publication, Tripoli, pp. 130.
- [28]. Rohlich, P. 1974, Geological map of Libya; 1:250,000 sheet, Al Bayda sheet NI34-15, explanatory booklet. Indust. Res. Cent., Tripoli, pp. 70.
- [29]. Desio, A. 1935, Studi geologici sulla Cirenaica, sul deserto Libico, sulla Tripolitania e sul Fezzan orientale. Missione scientifica della R. Accad. d'Italie a Cufra, (1931), Roma. vol. 1. 480p.
- [30]. Pietersz, C.R. 1968, Proposed nomenclature for rock units in Northern Cyrenaica. In geology and archaeology of northern Cyrenaica, Libya. Soc. Libya, Tripoli, p. 125-130.
- [31]. Lindholm, R.C. 1987, A practical approach to sedimentology: Boston, Mass., London, Sydney, Wellington: Allen & Unwin. pp. 279.
- [32]. Kasturi B., Subhashish D. 2018, Paleocurrent Analysis of Kolhan Basin: Implications to Paleogeographic Reconstructions. Curr Trends Biomedical Eng & Biosci. 2018; 13(1): 555854. DOI:10.19080/CTBEB.2018.13.555854.
- [33]. Potter, P.E. 1978, Petrology and chemistry of modern Big River Sands. J. Geol., 86: p. 423-449.



Dr. Omar B. Elfigih holds MSc. and Ph.D. degrees in petroleum geology from the Memorial University of Newfoundland-Canada. He has been in the oil industry from 1985 till 2009 with the Arabian Gulf Oil Company (AGOCO) Benghazi-Libya, he has focused on the multidisciplinary integration of geological data used in well-site operations and prospect generation in various concessions in the Ghadames Basin, NW Libya, and as a technical geological supervisor for the exploration group of the Ghadames (Hamada) Basin.

Dr. Elfigih worked for BP company- Libyan branch as a consultant in petroleum geology in some of their concessions in NW Libya. He joined the Department of Earth Sciences at the University of Benghazi since 2009 and taught many courses; stratigraphy, sedimentology, structure geology, petroleum geology, basin analysis, and applied sedimentology for both undergraduate and postgraduate programs. Supervising many MSc. theses in the field of petroleum geology. He was the head of the Earth Sciences Department, Faculty of Science, the University of Benghazi from Oct. 2014 to Oct. 2016. He is now a professor in petroleum geology at the Department of Earth Sciences-University of Benghazi. Head of scientific affairs at the University of Technical Research for Engineering Sciences (UTRES).

Dr. Elfigih is a member of many geological societies; including the Earth Sciences Society of Libya (ESSL), the Geological Association of Canada (GAC), and the American Association of Petroleum Geologists (AAPG).



Mr. Osama A. Alshireef was born in Benghazi-Libya in August 1986. He received his BSc. in geology from the University of Benghazi in 2010, and MSc. in applied sedimentology from the University of Benghazi in 2021. **Mr. Alshireef** was employed by the Sirte Oil Company in 2014 as a wellsite geologist, he has diversified experience in geological operations, and reservoir geology, successfully working in the most prominent oil and gas basin in Libya (Sirt Basin). **Mr. Alshireef's** research interests include sequence stratigraphy, sedimentology, facies analysis, and computer applications.